

**Influence of cyclonic and anti-cyclonic eddies on plankton ~~biomass,~~  
~~activity and diversity~~ in the southeastern Mediterranean Sea during late  
summertime**

Formatted: Font: 14 pt

Natalia Belkin<sup>1\*</sup>, Tamar Guy-Haim<sup>1</sup>, Maxim Rubin-Blum<sup>1</sup>, Ayah Lazar<sup>1</sup>, Guy Sisma-  
5 Ventura<sup>1</sup>, Rainer Kiko<sup>2</sup>, Arseniy R. Morov<sup>1</sup>, Tal Ozer<sup>1</sup>, Isaac Gertman<sup>1</sup>, Barak Herut<sup>1</sup>,  
Eyal Rahav<sup>1\*</sup>

<sup>1</sup> Israel Oceanographic and Limnological Research, Haifa, Israel

<sup>2</sup> Sorbonne Université, Laboratoire d'Océanographie de Villefranche, Villefranche-sur-  
Mer, France

Correspondence to: [eyal.rahav@ocean.org.il](mailto:eyal.rahav@ocean.org.il), [belkin@ocean.org.il](mailto:belkin@ocean.org.il)

**Abstract.** Planktonic food-webs were studied contemporaneously in a mesoscale cyclonic (upwelling, ~13 months old) and an anti-cyclonic (down-welling, ~2 months old) eddies, as well as in an uninfluenced-background situation in the oligotrophic southeastern Mediterranean Sea (SEMS) during late summer 2018. We show that integrated nutrients concentrations were higher at the cyclone compared to the anti-cyclone or the background stations by 2-13 fold. Concurrently, *Synechococcus* and *Prochlorococcus* were the dominant community component abundance-wise in the oligotrophic anti-cyclone (~300x10<sup>10</sup> cells m<sup>-2</sup>). In the cyclone, pico- and nanoeukaryotes such as dinoflagellates, Prymnesiophyceae and Ochrophyta contributed substantially to the total phytoplankton abundance (~14x10<sup>10</sup> cells m<sup>-2</sup>) which was ~65% lower in the anti-cyclone/background stations (~5x10<sup>10</sup> cells m<sup>-2</sup>). Primary production was highest in the cyclonic eddy (191 mg C m<sup>-2</sup> d<sup>-1</sup>) and was 2-5 fold lower outside the eddy area. ~~The calculated doubling time of phytoplankton was 3 days in the cyclone and 5-10 days at the anti-cyclone/background stations, further reflecting the nutritional differences between these environments.~~ Heterotrophic prokaryotic cell-specific activity was highest in the cyclone (~10 fg C cell<sup>-1</sup> d<sup>-1</sup>), while the least productive cells were found in the anti-cyclone (4 fg C cell<sup>-1</sup> d<sup>-1</sup>). ~~The calculated doubling time of heterotrophic bacteria were 1.4 days in the cyclone and 2.5-3.5 days at the anti-cyclone/background stations.~~ Total zooplankton biomass in the upper 300 m was tenfold higher in the cyclone compared with the anti-cyclone or background stations (1337 vs. 112-133 mg C m<sup>-2</sup>, respectively). Copepod diversity was much higher in the cyclone (44 species), compared to the anti-cyclone (6 small-size species). Our results highlight that cyclonic and anti-cyclonic eddies show significantly different community compositions and food-web dynamics in oligotrophic environments, with cyclones representing productive oases in the marine desert of the SEMS.

**Keywords:** Southeastern Mediterranean Sea; Cyclonic eddy, Anti-cyclonic eddy; Primary productivity; Bacterial productivity; Phytoplankton; Zooplankton; ~~PERLE~~.

**Running page head:** Cyclone and anticyclone eddies affect plankton

Formatted: Font: Not Bold

Formatted: Justified, Space Before: 12 pt, After: 0 pt

## 1 Introduction

The southeastern Mediterranean Sea (SEMS) is an ultra-oligotrophic marine system (Berman et al., 1984) with low and patchy standing stocks of phytoplankton (Christaki, 2001; Efrati et al., 2013) and zooplankton (Pasternak et al., 2005; Siokou-Frangou et al., 2002). Phytoplankton are bottom-up controlled by N and P (Tanaka et al., 2011; Zohary et al., 2005) and heterotrophic bacteria are limited by P (Sala et al., 2002; Thingstad et al., 2005; Zohary and Robarts, 1998), dissolved organic P (DOP, Van Wambeke et al. 2002; Djaoudi et al. 2018; Sisma-Ventura and Rahav 2019) and/or dissolved organic C (DOC, Hazan et al. 2018; Rahav et al. 2019). Phytoplankton is mostly comprised of cyanobacteria and pico-sized microbial eukaryotes with a high surface-area-to-volume ratio (Berman-Frank and Rahav, 2012; Ignatiades et al., 2002) that enables a faster nutrient uptake from the environment (Campbell and Vaultot, 1993). The low phytoplankton standing stocks lead to low primary production rates of  $32\text{--}60\text{ gC m}^{-2}\text{ y}^{-1}$  (López-Sandoval et al., 2011; Psarra et al., 2000). Zooplankton biomass is usually coupled with that of the phytoplankton and is mostly comprised of mesozooplankton lineages that feed on pico-phytoplankton (Dolan and Marrasé, 1995; Pitta et al., 2001) or other mesozooplankton (Christou, 1998; Pasternak et al., 2005).

Alterations in plankton biomass or activity from their typically-low values can be found episodically in the SEMS at distinct hydrologic discontinuities such as cyclonic (upwelling) and anticyclonic (down-welling) eddies (Christaki et al., 2011; Groom et al., 2005; Rahav et al., 2013). These geostrophically balanced mesoscale structures can span tens to hundreds of kilometers in diameter (Groom et al., 2005; Robinson and Golnaraghi, 1994). These high-energy eddies may retain plankton communities over time-scales of weeks to months (Christaki et al., 2011; Menna et al., 2012; Rahav et al., 2013) and affect limiting nutrient levels at the euphotic zone (Condie and Condie, 2016). Therefore, the transport of potential and kinetic energy, nutrients and biota by eddies (cyclonic or anti-cyclonic) may alter phytoplankton and zooplankton biomass and activity (Allen et al., 1996; Falkowski et al., 1991).

In this study, we report the results of physical, chemical and biological samplings of two contrasting sites in the SEMS deep waters: cyclonic and anti-cyclonic eddies, as well as a background, uninfluenced station. We sampled these stations at the end of

summer when the most oligotrophic conditions prevail in the photic layer (Kress et al., 2014; Rahav et al., 2019). We hypothesized that the upward advection of deep, and relatively cold nutrient-rich water within the cyclonic eddy enhance primary production, as well as the biomass of picoeukaryotes and zooplankton. On the contrary, down-welling circulation at the anti-cyclonic eddy yields ultra-oligotrophic conditions, even more than those of the background waters of the SEMS, leading to low phytoplankton biomass and production, the predominance of cyanobacteria, and low zooplankton biomass.

## 2 Methods

### 2.1. Study area and seawater collection

Water samples were collected during 9-11 October 2018 on-board the R/V *Bat-Galim* in three distinct water habitats: 1) Core of an anti-cyclonic eddy (Lat. 32.14 N, Lon. 33.59 E); 2) Core of a cyclonic eddy (Lat. 33.16 N, Lon. 33.86 E); and 3) A station uninfluenced by eddy circulation (hereafter referred to as 'background', Lat. 32.95 N, Lon. 34.46 E) (**Figure 1A**). The eddy's core locations were determined a few days prior to the cruise and were updated until the morning of the cruise by maps created with the Angular Momentum Eddy Detection and tracking Algorithm (AMEDA) (Le Vu et al., 2018) applied on AVISO/CMEMS Sea Surface Height (SSH) data, which were produced especially for this mission. This algorithm tracks individual eddies and accounts for successive merging and splitting incidents between eddies. It also corrects for cyclostrophic balance of the surface velocity field, which allows a better representation of intense eddies (Ioannou et al., 2019). A more detailed characterization of the physical structure of the water column inside/outside the different cores was collected during the cruise and a few days afterward using a SeaExplorer glider equipped with temperature and salinity sensors (see below). The cruise was part of a cooperation with the 'Pelagic Ecosystem Response to dense water formation in the Levant' (PERLE) campaign, which is one of the three operations of the MERMEX (Marine Ecosystem Response in the Mediterranean EXperiment, <https://mERMEX.mio.univ-amu.fr/>) project. As such, it coincided with the project's standard sampling protocols.

Seawater was sampled using Niskin bottles (8 L each) mounted on a rosette equipped with a CTD (Seabird 9 Plus) and a fluorometer (Sea-Point). Five to six water

depths were sampled in each station which represented the main oceanographic features within the water column derived from real-time CTD and fluorometer data: the surface (2 m), the bottom of the mixed layer depth (30-60 m), the deep chlorophyll-*a* area (60-165 m), and bottom of the photic layer (180 m). An additional offshore station uninfluenced by eddy circulation (station THOMO1) was sampled in a parallel cruise at the SEMS on the same date as our study in larger details (11 depths within the photic layer, Reich et al., 2021, 2022). The chemical and chlorophyll-*a* profiles were not significantly different between the THOMO1 and our background stations (Kruskal-Wallis One Way Analysis of Variance on Ranks,  $P > 0.05$ , **Figure S1**), thus giving credibility to our measurements which comprised only 5-6 depths at the photic layer. Meso-zooplankton were sampled using vertical WP2 hauls ( $\varnothing$ -57cm, 50- $\mu$ m mesh-size, Hydro-Bios, Germany) hoisted at 0.5 m s<sup>-1</sup> from 300 m to the water surface during nighttime (19:00-06:00). The southeastern Mediterranean Sea is an extremely oligotrophic region, with very low zooplankton densities, especially in the large-size fraction (Koppellmann et al., 2009). It was therefore stressed that the standard 200- $\mu$ m is underestimating the mesozooplankton abundance and community structure in this region (Feliú et al., 2020) and therefore we used the 50- $\mu$ m mesh-size. Filtered volume was measured using a mechanical flow meter (Hydro-Bios, Germany). The raw oceanographic data is publicly available at the ISRAMAR oceanographic database website ([isramar.ocean.org.il](http://isramar.ocean.org.il)).

## **2.2. SeaExplorer glider mission to characterize the physical characteristics of the water column (upper 700 m) within and outside the cores area**

An autonomous underwater vehicle (SeaExplorer glider, ALSEAMAR) equipped with a SeaBird CTD was deployed at the southernmost sampling station (at the core of the anti-cyclone). The glider collected the temperature and salinity characteristics across the upper 700 m in a very high spatiotemporal coverage during ~18 days. The glider performed a total of 146 dives on its route northwards, yielding 292 quasi vertical profiles (see the glider track in **Figure 1A**).

## **2.3. Inorganic nutrients**

Nutrient concentrations were determined using a three-channel segmented flow auto-analyzer system (AA-3 Seal Analytical) as described in Sisma-Ventura and Rahav (2019). The detection limit (3 times the standard deviation of 10 measurements of low

nutrient seawater), was  $0.08 \mu\text{mol L}^{-1}$  for  $\text{NO}_2+\text{NO}_3$  ( $\text{NO}_x$ ),  $0.008 \mu\text{mol L}^{-1}$  for  $\text{PO}_4^{3+}$  and  
135  $0.05 \mu\text{mol L}^{-1}$  for  $\text{Si}(\text{OH})_4$ . Analysis reproducibility was determined using MOOS 3 ( $\text{PO}_4^{3+}$ ,  
 $\text{NO}_x$  and  $\text{Si}(\text{OH})_4$ ), VKI 4.1 ( $\text{NO}_x$ ) and VKI 4.2 ( $\text{PO}_4^{3+}$  and  $\text{Si}(\text{OH})_4$ ) certified references  
materials (CRM). Results were accepted when measured CRM's were within  $\pm 5\%$  from  
the certified values.

#### 2.4. Chlorophyll-*a* and algal photosynthetic pigments markers

140 Seawater samples (500 mL) were concentrated on deck using a Whatman GF/F  
( $\sim 0.7 \mu\text{m}$  pore size) at low pressure ( $<150$  mbar) for chlorophyll-*a* (chl-*a*) analysis. The  
filters were placed in glass vials and frozen in the dark at  $-20^\circ\text{C}$  until analysis. Chl-*a*  
pigment was extracted overnight in cold acetone (90%) in the dark and determined by the  
non-acidification method (Welschmeyer, 1994) using a Turner Designs (Trilogy)  
145 fluorometer. The chl-*a* reads were then calibrated against the *in situ* fluorimeter mounted  
on the rosette, using a linear regression equation ( $n=19$ ,  $r=0.95$ ,  $p<0.001$ ). For biomarker  
photosynthetic pigments analyses, 8 L of seawater were concentrated on GF/Fs, and kept  
frozen at  $-20^\circ\text{C}$  in aluminum foil until analysis. High-Performance Liquid  
Chromatography (HPLC) was used to identify and quantify the biomarker photosynthetic  
150 pigments concentrations using a 40 min Ethyl-acetate methanol gradient method (Jeffrey  
et al., 1997). Pigments were extracted in 90% acetone for 24 h in  $4^\circ\text{C}$ . The extracts were  
filtered through a  $0.45 \mu\text{m}$  Teflon syringe filter and transferred into glass HPLC vials. The  
extracts ( $100 \mu\text{L}$ ) were analyzed using an Agilent 1220 HPLC system equipped with a  
diode array and fluorescence detectors. Selected pigment standards (DHI Labs) were used  
155 for verification of the spectra and retention times.

#### 2.5. Pico/nano-phytoplankton and heterotrophic prokaryotic abundance

Samples (1.8 mL) were fixed with glutaraldehyde (final concentration 0.02% v:v, Sigma-  
Aldrich G7651), frozen in liquid nitrogen, and later stored at  $-80^\circ\text{C}$  until analysis within a  
week. The abundance of autotrophic pico- and nano-eukaryotes, *Synechococcus* and  
160 *Prochlorococcus* and other heterotrophic prokaryotes (bacteria and archaea) was  
determined using an Attune® Acoustic Focusing Flow Cytometer (Applied Biosystems).  
Heterotrophic prokaryotes (hereafter refer to as heterotrophic bacteria, BA) were stained  
with SYBR Green (Applied Biosystems). Total phytoplankton and microbial biomass were

calculated according to Houlbrèque et al. (2006). Phytoplankton and microbial doubling  
time estimates were calculated by dividing the integrated phytoplankton biomass by  
integrated primary and bacterial production, respectively (Kirchman, 2012).

## 2.6. Primary production (PP)

Triplicate water samples (50 mL) were spiked upon sampling with 5  $\mu\text{Ci}$  of  $\text{NaH}^{14}\text{CO}_3$   
(Perkin Elmer, specific activity 56  $\text{mCi mmol}^{-1}$ ) (Steemann-Nielsen, 1952). The samples  
were incubated for 24 h under *in situ* natural illumination and surface temperature in a  
flow-through tank on deck covered with a light screening mesh. The incubations were  
terminated by filtering the spiked seawater through GF/F filters (Whatman, 0.7  $\mu\text{m}$  pore  
size) at low pressure ( $\sim 50$  mmHg). Measurements for the added activity and dark controls  
were also performed. The filters were placed overnight in 5 mL scintillation vials  
containing 50  $\mu\text{l}$  of 32% hydrochloric acid to remove excess  $^{14}\text{C}$ , after which 5 mL of  
scintillation cocktail (Ultima-Gold) were added. Radioactivity was measured using a TRI-  
CARB 2100 TR (Packard) liquid scintillation counter.

Note that the rates considered here only account for the particulate PP and not the dissolved  
fraction, and therefore the total PP may be underestimated (by average  $\sim 20\%$  in  
oligotrophic seas, Marañón et al. 2005). Yet, we surmise that if underestimation did occur,  
it was similar in all stations sampled. Moreover, it is to be noted that due to the relatively  
low number of depths sampled in each station ( $n=5-6$ ), it is possible that some peaks in PP  
(e.g., at the subsurface) may have been overlooked, resulting in underestimation of the  
integrated values.

## 2.7. Bacterial production (BP)

Prokaryotic (bacteria and archaea) heterotrophic production (hereafter refer to as BP) was  
estimated using the  $^3\text{H}$ -leucine incorporation method (Perkin Elmer, specific activity 100  
 $\text{Ci mmol}^{-1}$ ). Three replicates (1.7 mL each) from each water depth were incubated in the  
dark (wrapped in aluminum foil) with  $\sim 10$  nmol hot leucine  $\text{L}^{-1}$  for 4 h (Rahav et al., 2019).  
Control treatments in which surface water was immediately added with 100  $\mu\text{l}$  of 100%  
trichloroacetic acid (TCA, 4  $^\circ\text{C}$ ) along with  $^3\text{H}$ -leucine were also carried in triplicates. The  
incubations were terminated with TCA and were later processed following the micro-  
centrifugation technique (Smith et al., 1992) and added with 1 ml of scintillation cocktail

(Ultima-Gold). The samples were counted using a TRI-CARB 2100 TR (Packard) liquid  
 195 scintillation counter. A conversion factor of 1.5 kg C mol<sup>-1</sup> per every mole leucine  
 incorporated was used (Simon et al., 1989).

## 2.8. Zooplankton biomass

Zooplankton samples were sieved through a 100-µm mesh and halved into two subsamples  
 200 using a plankton sample splitting box (Motoda, 1959). One subsample was kept at -20 °C  
 for biomass analysis and the second subsample was preserved in 99.8% ethanol for  
 molecular analysis- (Harris et al., 2000). In the lab, the collected samples were thawed and  
 filtered using pre-combusted GF/C filters and weighed after drying in 60 °C for 24 h to  
 obtain dry weight (DW), and after 4 hours in 500 °C to measure ash weight and obtain  
 carbon content as ash-free dry weight (AFDW).

205 The grazing impact of zooplankton on phytoplankton was calculated as the relative portion  
 of zooplankton carbon biomass from the total pico/nanophytoplankton biomass.

## 2.9. Zooplankton carbon and nutrient demand estimates

Zooplankton carbon demand (ZCD in mg C m<sup>-3</sup> d<sup>-1</sup>) was calculated based on measured  
 biomass and growth rate estimates (following the cross-Mediterranean estimates in Feliú  
 210 et al., 2020):

$$ZCD = C_{zoo} \times F_R$$

Where,  $C_{zoo}$  is the carbon concentration of zooplankton (in mg C m<sup>-3</sup>) and  $F_R$  is the food  
 ratio, defined as the amount of food consumed per unit of biomass per day (d<sup>-1</sup>), calculated  
 as:

$$F_R = \frac{g_Z + r}{A}$$

Where,  $g_Z$  is the growth rate,  $r$  is the weight specific respiration and  $A$  is assimilation  
 efficiency.  $r$  and  $A$  were set to 0.16 d<sup>-1</sup> following Alcaraz et al. (2007) and 0.7 following  
 Nival et al. (1975).  $g_Z$  was calculated following Zhou et al. (2010):

$$g_Z(C_{zoo}, T, Chl.a) = 0.033 \left( \frac{Chl.a}{Chl.a + 205e^{-0.125T}} \right) e^{0.09T} W_{zoo}^{-0.06}$$



220 Where T is seawater temperature (average value for 0-300 m: background 18.8 °C, cyclone  
17.8 °C, anti-cyclone 20.0 °C), chl-a is food availability (mg C m<sup>-3</sup>) estimated from the  
integrated chl-a values. W<sub>ZOO</sub> is the average carbon concentration per zooplankter, set to  
0.01072 mg C ind<sup>-1</sup> based on data collected from the background station in 2019-2020  
(Guy-Haim, unpublished data). Phytoplankton was considered as food following Calbet et  
225 al. (1996). ZCD was compared to the phytoplankton stock and to primary production to  
estimate the potential clearance of phytoplankton by zooplankton.

N and P excretion and oxygen consumption rates for an average zooplankter with weight  
W<sub>ZOO</sub> were estimated using the multiple regression model by Ikeda, (1985) based on carbon  
weight and temperature:

230 
$$\ln Y = a_0 + a_1 \ln W_{ZOO} + a_2 T$$

Where Y represents N or P excretion or oxygen uptake.  $a_0$ ,  $a_1$  and  $a_2$  are constants specific  
to each metabolic process (respiration, ammonia and phosphate excretion). Total N and P  
excretion were obtained by multiplying the obtained rate with the zooplankton biomass  
measured at each station. Zooplankton's contribution to nutrient regeneration (in %) was  
235 estimated by comparison to primary production converted to N and P requirements. To this  
end, we used C:N:P ratios different than the 'typical' Redfield 106:16:1 stoichiometry as  
previously reported in the ultra-oligotrophic Levantine basin water (Pujo-Pay et al., 2011).  
Where, the POC:PN is 5.4:1 (instead of ~6.6:1) and POC:PP is 116:1 (instead of 106:1).  
Respiration was converted to respiratory carbon lost assuming a respiratory quotient of  
240 0.97 following Ikeda et al. (2000) and used as a carbon requirement for zooplankton  
metabolism.

## 2.10. Molecular diversity of microbial and zooplankton communities

Seawater (8 L) was filtered using a peristaltic pump onto Supor membrane filters (0.2 µm,  
47 mm, PALL, USA) and placed immediately in PowerWater DNA bead tubes (Qiagen,  
245 USA), flash-frozen in liquid nitrogen and preserved at -20 °C (n=1 per depth except in  
selected samples where n=2). DNA was extracted with the DNeasy PowerWater Kit  
(Qiagen, USA), following the standard protocol including an extra heating step at 65 °C  
for 10 min as recommended by the manufacturer for samples containing algae. Ethanol-

250 preserved zooplankton samples were sieved using a 100- $\mu$ m Nitex sieve, washed with  
distilled water to remove ethanol residuals, and homogenized by vigorous vortex and  
pipetting. Genomic DNA was extracted using DNeasy Blood and Tissue Kit (Qiagen,  
USA) following the manufacturer's instructions.

DNA was amplified with the following primer sets amended with CS1/CS2 tags: i) The V4  
region of the 16S rRNA gene (ca. 300 bp), 515Fc/806Rc, (Apprill et al., 2015; Parada et  
255 al., 2016); ii) the 18S rRNA gene (200-500 bp); 1391F, EukBr, (Amaral-Zettler et al.,  
2009), and iii) the mitochondrial cytochrome *c* oxidase I (COI) gene (ca. 300 bp),  
mlCOIintF, jgHCO2198. Library preparation from the PCR products and sequencing of  
2x250 bp Illumina MiSeq reads was performed by HyLabs (Israel). The COI and 18S  
rRNA gene amplicon reads were submitted to NCBI Sequence Read Archive BioProject  
260 PRJNA667077.

#### **2.11. Bioinformatic analyses of marker gene amplicons**

Demultiplexed paired-end reads were processed in QIIME2 V2020.6 environment (Bolyen  
et al., 2019). Reads were truncated based on quality plots, checked for chimeras, merged  
and grouped into amplicon sequence variants (ASVs) with DADA2 (Callahan et al., 2016),  
265 as implemented in QIIME2. The 16S and 18S rRNA amplicons were classified with scikit-  
learn classifier that was trained on the Silva 138 database or BLAST against the Silva 138  
database (0.9 minimum identity cutoff, performed best for the analyses of 18S gene  
amplicons of microbial zooplankton). COI amplicons were classified with BLAST (0.9  
minimum identity cutoff) against the merged NCBI/BOLD database (Heller et al., 2018),  
270 which was transformed into QIIME2 format. Downstream statistical analyses, calculation  
of alpha diversity indices (the richness estimator ACE - Abundance-based Coverage  
Estimator, and the biodiversity estimators Shannon and Simpson), beta diversity (non-  
metric multidimensional scaling, NMDS, based on the Bray-Curtis dissimilarity) and  
plotting were performed in R (R Core Team, 2018) using packages phyloseq (McMurdie  
275 and Holmes, 2013), ampvis2 (Andersen et al., 2018) and ggplot2 (Wickham, 2011).  
Mitochondrial and chloroplast sequences were removed from the 16S rRNA amplicon  
dataset, the relative abundance of microbial eukaryotes was estimated following the  
removal of metazoan 18S rRNA sequences.

## 2.12. Statistical analyses

Nutrients, pico-phytoplankton, heterotrophic bacteria, as well as primary and bacterial production were vertically integrated using the trapezoidal rule, and compared between sampling locations ('background', 'anti-cyclonic eddy' and 'cyclonic eddy') using a one-way ANOVA and a Fisher LSD means comparison test ( $\alpha=0.05$ ). Statistically significant differences ( $p<0.05$ ) were labeled with different letters. DESeq2 (Love et al., 2014) was used to evaluate the differential abundance of bacterioplankton ASVs at the DCM. Note that the limited number of samples collected in each hydrologic discontinuity per depth ( $n=1-2$ ), contrary to integrated calculations which pool 4-6 measurements from the upper 180 m, restricted our ability to run additional statistical comparisons between locations. We discuss these caveats below and also compare our findings to other relevant studies from the Mediterranean Sea (i.e., BOUM and ISRALEV campaigns) and elsewhere (e.g., the Eastern Indian Ocean, Waite et al. 2007), as well as compare our nutrients and chl-a profiles to a parallel cruise held at the same time of our study nearby (**Figure S1**).

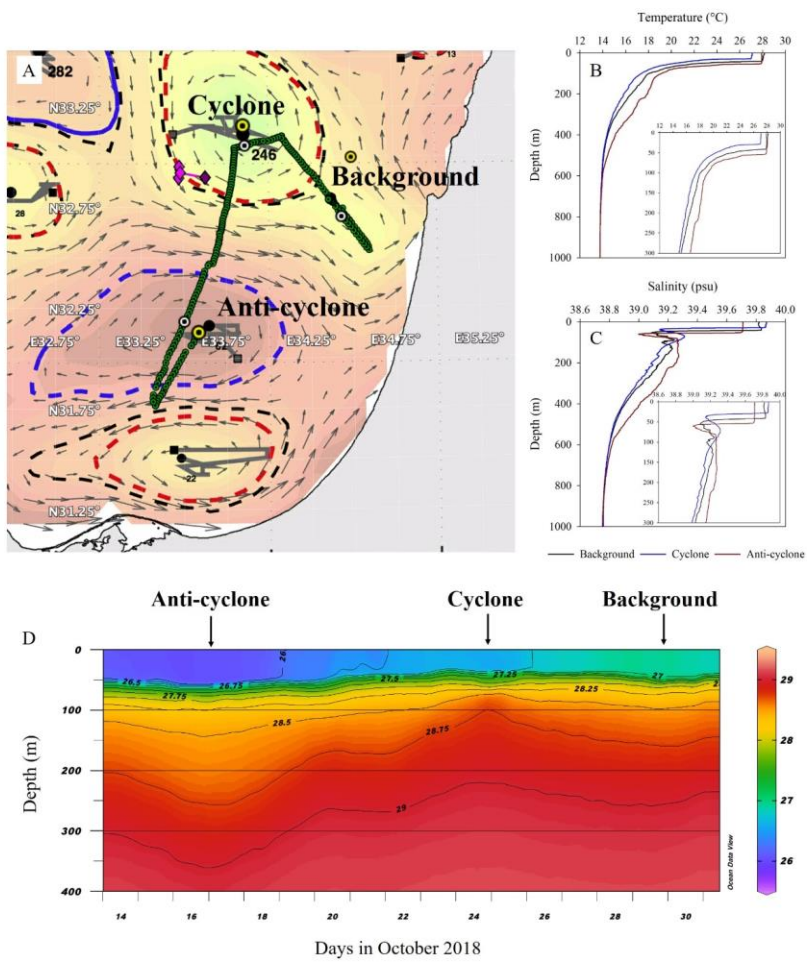
## 3 Results

The AMEDA algorithm shows a chain of cyclonic and anti-cyclonic eddies at the SEMS (**Figure 1A**). The stations were selected to sample the cores of the southern cyclonic and anti-cyclonic eddies offshore the Israeli coast, as well as background stations. The anti-cyclone, later identified in the DYNED atlas as anti-cyclone #12683, was created from a meander of the along-shore current in the southeastern corner of the basin in early August 2018, just 62 days prior to the cruise. It mixed warm water from the eastern sea margin (**Figure S2A**). The cyclonic eddy was created in early February 2018, 246 days before the cruise. Later, when the DYNED atlas was extended to include 2018, it was identified as cyclonic eddy #11988 that was created more than a year earlier, mid-September 2017-  
(Figure S2). It was split from cyclone #11310 located south of Cyprus and migrated to the Haifa area (Figure S2). The easternmost SEMS. Profiles of Argo floats (#6903221 and #6903222) localized within cyclone #11310 showed that it brought denser, colder and saltier water upwelled on the southern Cyprus coast (**Figure S2A**). At the time it was sampled it is characterized as a cold-core cyclone, colder than its surrounding waters (**Figure S2B**).

Formatted: Default Paragraph Font

The sea surface temperature (SST) in the anti-cyclonic eddy and background stations was the warmest ( $\sim 28^{\circ}\text{C}$ ), while a lower temperature was recorded in the cyclonic eddy ( $\sim 27^{\circ}\text{C}$ ) (**Figure 1B; Figure S3**). Further, down to 550 m the highest water temperatures were recorded in the anti-cyclonic eddy (a positive anomaly compared to the background), and the coldest temperatures were recorded in the cyclonic eddy (a negative anomaly). From  $\sim 550$  m to 1000 m depth the water temperature in all sampling stations was the same and constant ( $\sim 14^{\circ}\text{C}$ ) (**Figure 1B; Figure S3**). Surface salinity ranged from 39.7 to 39.8 psu and decreased to 38.8 psu at 550 m in all sampling sites (**Figure 1C; Figure S3**). The concurrent potential density anomaly derived from a detailed glider mission that occurred the following week to our cruise shows that the sampling stations were within the cores of the two distinct hydrologic discontinuities (**Figure 1D; Figure S3**). The Levantine Intermediate Water (LIW), characterized by high salinity and relatively warm temperatures, was evident at  $\sim 70$  m in the up-welling cyclonic eddy,  $\sim 130$  m in the background station, and  $\sim 170$  m at the down-welling anti-cyclonic site (**Figure 1C; Figure S3**). This means that at the core of the cyclone, the LIW mass was uplifted to a relatively narrow layer (50-80 m; core at 75m) while in the core of anti-cyclone the LIW was much wider and deeper (80-240 m; core 175 m) due to convergence of currents (**Figure S3**).

$\text{NO}_2^- + \text{NO}_3^-$  ( $\text{NO}_x$ ) and orthophosphate ( $\text{PO}_4^{3+}$ ) concentrations were close to, or below, the detection limit of conventional analytical methods at all stations in the upper 100 m, while  $\text{Si}(\text{OH})_4$  levels were always above the detection limit (**Figure 2A-C, Table S1**). Nevertheless, marked differences were observed in the integrated nutrient values between sites at the photic layer (0-180 m), with 13-fold higher  $\text{NO}_x$ , 2.5-fold higher  $\text{PO}_4^{3+}$  and 1.5-fold higher  $\text{Si}(\text{OH})_4$  in the cyclonic eddy compared with the anti-cyclone (**Table 1**). Integrated N:P ratios at the background and anti-cyclone stations were lower than the Redfield ratio (15:1 and 9:1, respectively), whereas at the cyclone N:P ratio was higher ( $\sim 48:1$ ) (**Table 1**). From 180 m and down to the nutricline shoulder ( $\sim 400$  m), all nutrient levels gradually increased. Where  $\text{NO}_x$ ,  $\text{PO}_4^{3+}$  and  $\text{Si}(\text{OH})_4$  were higher by 45%, 90% and 100% in the cyclonic eddy than the anti-cyclonic eddy, respectively (**Figure 2A-C, Table S1**).



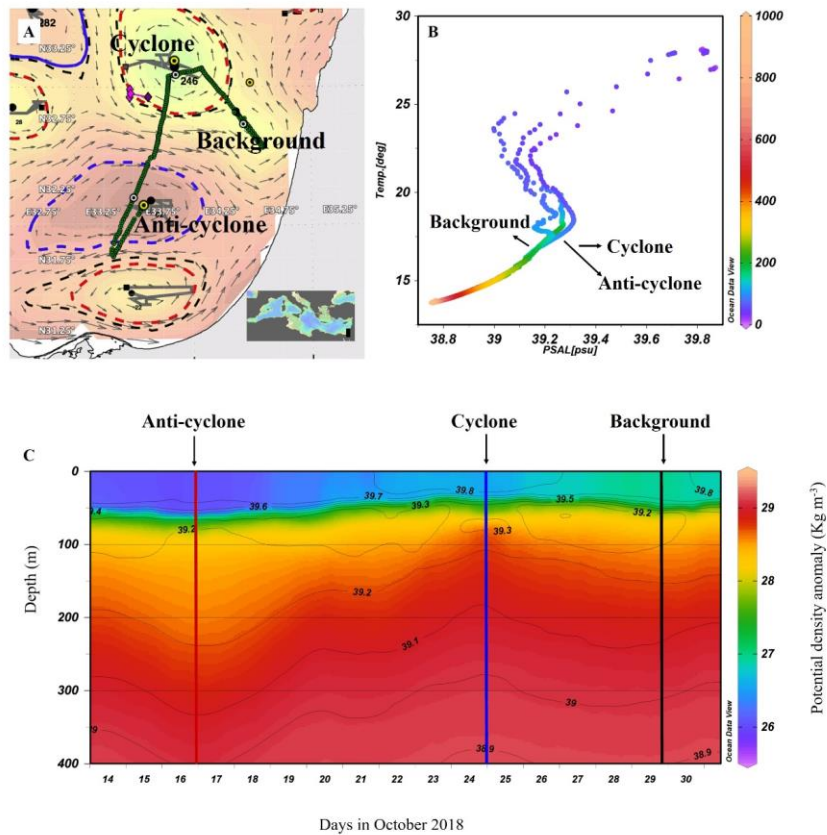


**Figure 1** – Altimetry map with eddies detected by the AMEDA algorithm created on the morning of the cruise (October 9, 2018), sampling stations (yellow marks) and a glider cruise-track (green dots) (A), the vertical profiles of temperature (B) and salinity (C) in cyclonic and anti cyclonic eddies and an uninfluenced background station at the southeastern Mediterranean Sea. Inserts show the upper 300 m of the water column. The temperature-salinity (T-S) diagram of the stations sampled (B), and the potential density anomaly derived from a glider mission (292 quasi-vertical profiles) held a few days after the cruise (October 13-31, 2018) (B-C). Contours on the density map show the corresponding isohalines.

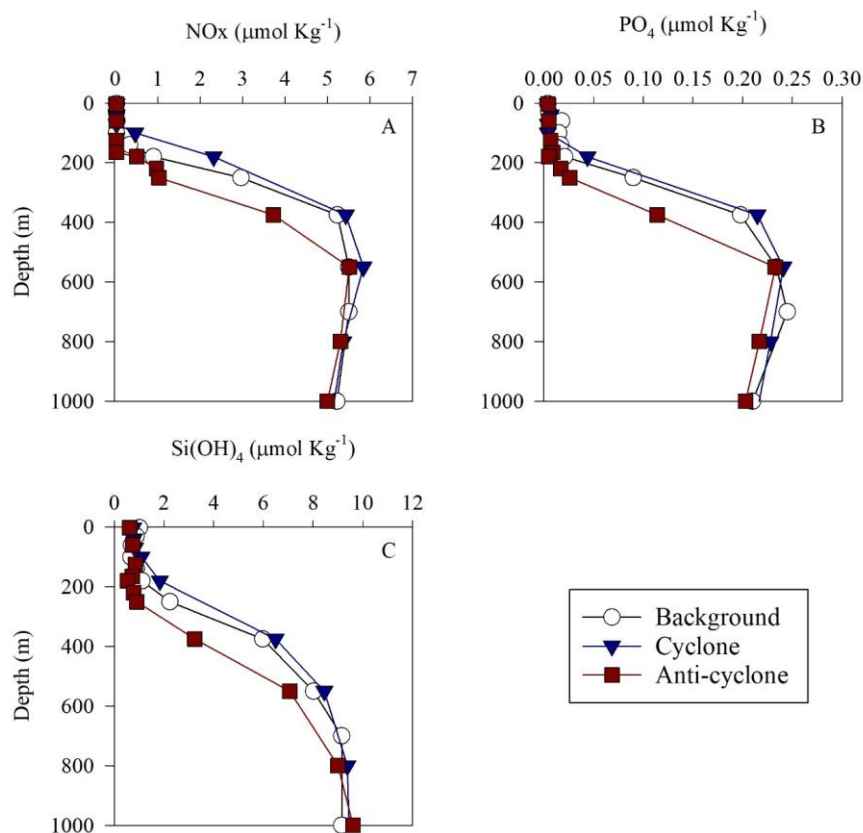


**Figure 2** – Vertical profile of NOx (A), PO<sub>4</sub><sup>3+</sup> (B) and Si(OH)<sub>4</sub> (C) in cyclonic (blue triangle) and anti-cyclonic (red square) eddies and an uninfluenced background station (white circle) in the southeastern Mediterranean Sea during October 2018.

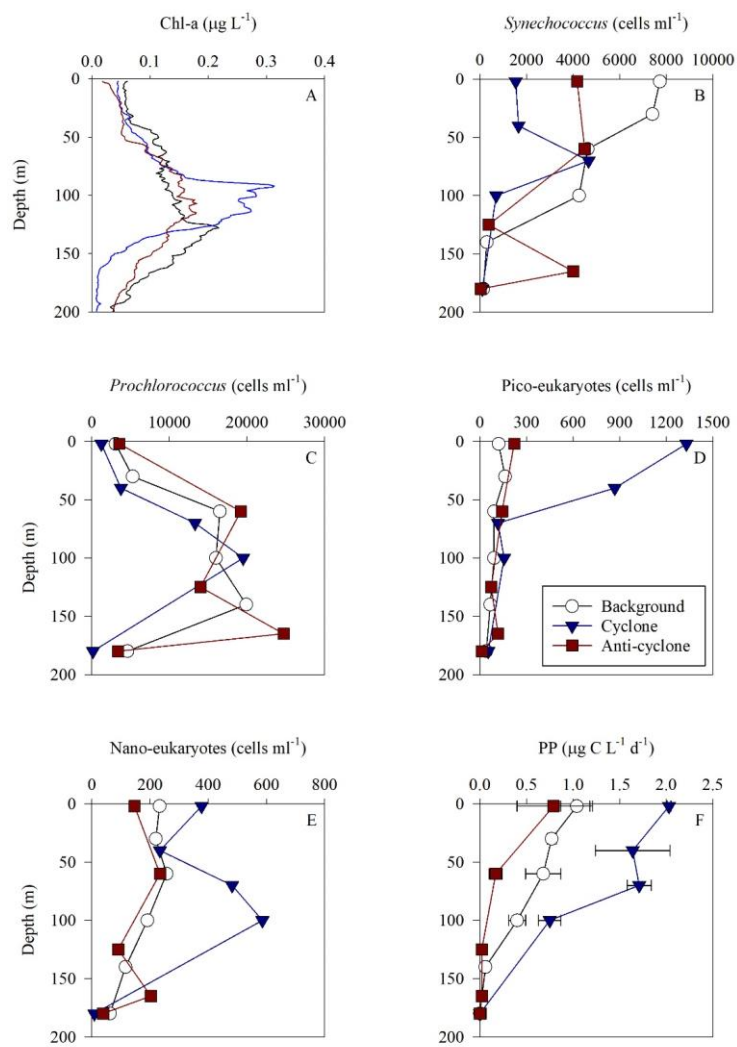
Following the elevated nutrient levels, integrated chl-*a* was highest at the cyclonic eddy and background stations (20.0-21.3 mg m<sup>-2</sup>), and lowest at the center of the ultra-oligotrophic anti-cyclonic eddy (17.9 mg m<sup>-2</sup>) (**Tables 1, S1**). The deep chlorophyll maximum (DCM) spread from 90-120 m in the cyclonic eddy, while a smaller DCM shoulder was observed in the anti-cyclonic eddy (~90-120 m) and at the background (~120-130 m) stations (**Figure 3A**). Nonetheless, the cyclone had the highest chl-*a* concentration

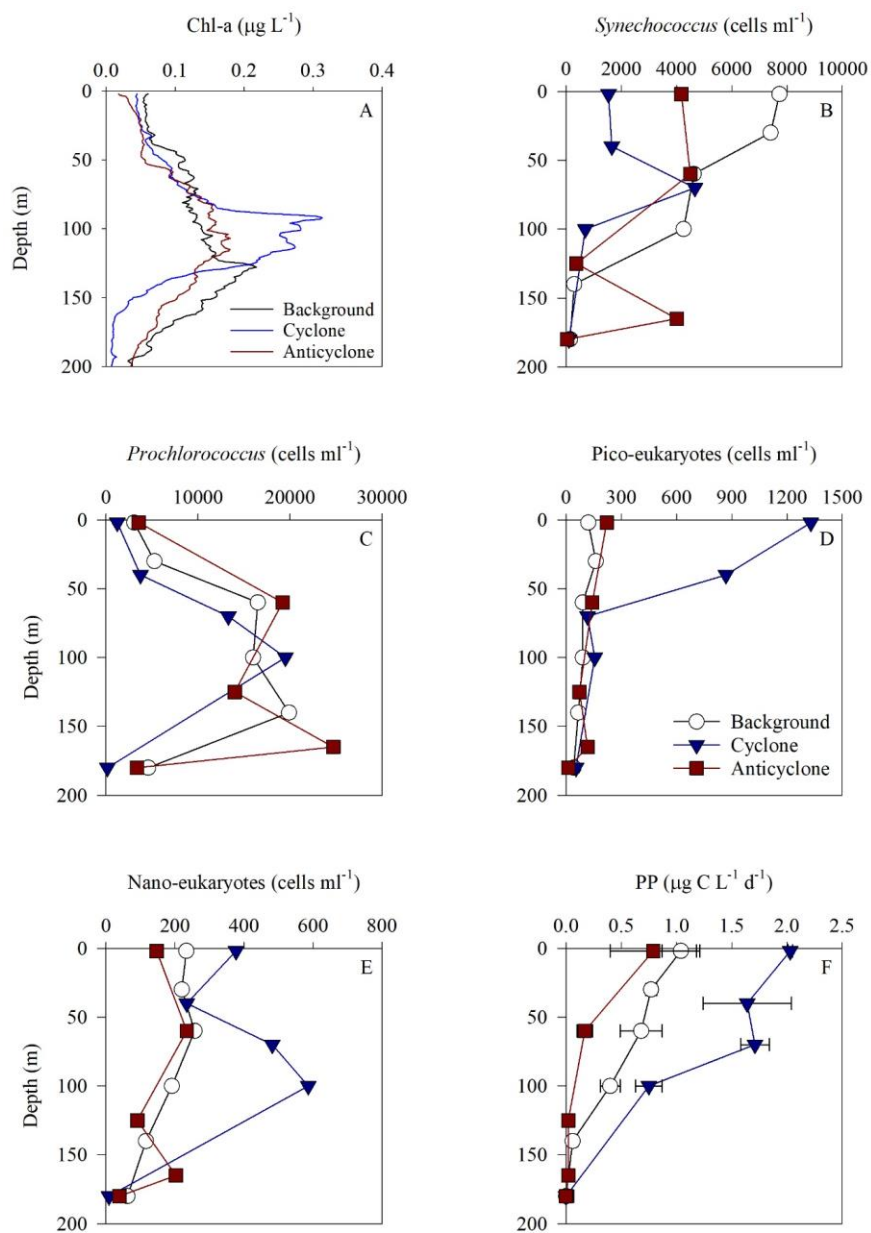
among all stations ( $0.31 \mu\text{g L}^{-1}$ ) while the DCM in the anti-cyclonic eddy had a weaker Chl-a signal ( $0.18 \mu\text{g L}^{-1}$ ) (**Figure 3A, Table S1**). *Synechococcus* was mostly found in the surface water of all stations, whereas *Prochlorococcus* occupied the DCM depths (**Figure 3B, C**). The highest cell abundance of these cyanobacteria was found at the background station ( $69 \times 10^{10}$  *Synechococcus* cells  $\text{m}^{-2}$ ) and in the anti-cyclone ( $270 \times 10^{10}$  *Prochlorococcus* cells  $\text{m}^{-2}$ ), while the lowest abundances were found in the cyclone ( $\sim 27 \times 10^{10}$  *Synechococcus* cells  $\text{m}^{-2}$  and  $\sim 160 \times 10^{10}$  *Prochlorococcus* cells  $\text{m}^{-2}$ ) (**Tables 1, S1**). Cyanobacterial read abundance based on amplicon sequencing supported these findings (**Figure 4**). The dominant bacterioplankton lineages in the photic zone included SAR86, Flavobacteriales, Puniceispirillales, Rhodospirillales, SAR11 (clade Ia) and others (**Figures 4, S4**). The abundance of pico- and nano-eukaryotic phytoplankton was higher at the cyclonic station ( $13.5 \times 10^{10}$  cells  $\text{m}^{-2}$ ) than the other stations sampled ( $\sim 5.5 \times 10^{10}$  cells  $\text{m}^{-2}$ ) (**Tables 1, S1**). Picoeukaryotes were mostly found in the surface water (top 50 m) and nanoeukaryotes were mostly found at the DCM depth (**Figure 3D, E**). Correspondingly, total pico-phytoplankton biomass was highest in the cyclonic eddy ( $597 \text{ mg C m}^{-2}$ ), which is 1.6-1.7-fold higher than at the background or anti-cyclonic stations (**Tables 1, S1**). 18S rRNA amplicon analyses indicated that at the photic depths mainly non-diatom microbial eukaryotes were dominant, such as dinoflagellates, Prymnesiophyceae and Ochrophyta (**Figures 5, S5**). Overall, the pico- and nano-eukaryotic populations were more diverse in the photic zone than in the deep waters, yet no major differences in alpha diversity parameters were observed between the stations (**Figure S6**).

Algal pigment analysis at the cyclone showed that the photosynthetic auxiliary pigments were mostly comprised of fucoxanthin ( $109 \text{ ng L}^{-1}$ ) - a pigment marker of diatoms, chrysophytes and some prymnesiophytes, and zeaxanthin ( $74 \text{ ng L}^{-1}$ ) - a pigment marker for green algae and cyanobacteria (**Figure S7**). At the anti-cyclonic eddy, fucoxanthin was also detected at the DCM, however, its concentration was lower by  $\sim 40\%$  ( $\sim 65 \text{ ng L}^{-1}$ ) while zeaxanthin concentration was slightly lower ( $\sim 64 \text{ ng L}^{-1}$ ) (**Figure S7**). As very few diatoms were detected by the 18S rRNA amplicon analysis, we surmise that the presence of fucoxanthin was most likely attributed to prymnesiophytes. Although the most considered diagnostic marker for prymnesiophytes is 19-hexanoyloxyfucoxanthin,

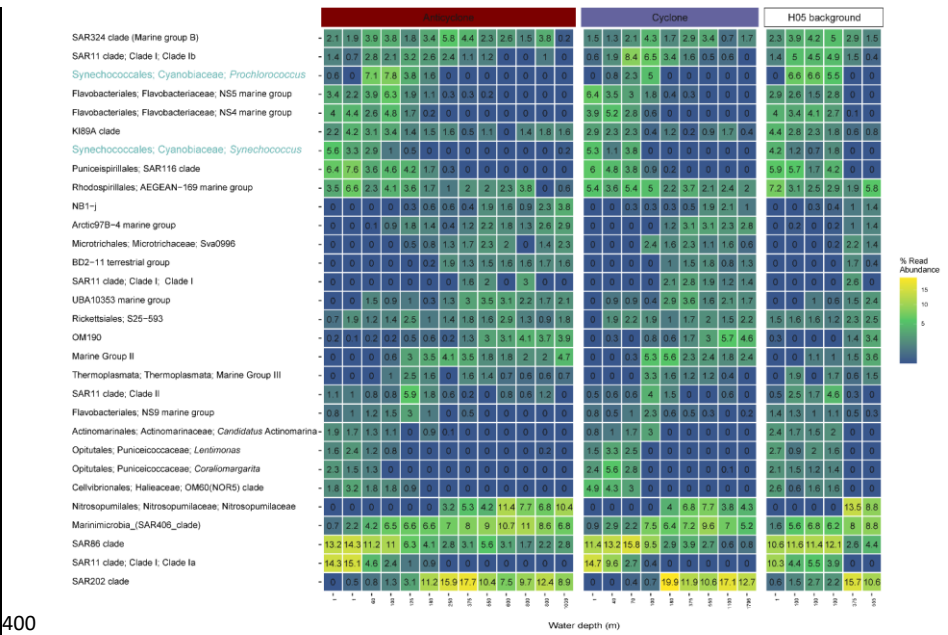


previous studies showed that fucoxanthin can also be used as their marker in absence of 19- hexanoyloxyfucoxanthin signals (Ansotegui et al., 2003).





395 **Figure 3** – Vertical profile of chlorophyll.a (A), *Synechococcus* (B), *Prochlorococcus* (C),  
pico-eukaryotes (D) nano-eukaryotes (E) and primary production rate (F) at the photic  
layer of cyclonic (blue triangle) and anti-cyclonic (red square) eddies and an uninfluenced  
background station (white circle) at the southeastern Mediterranean Sea during October  
2018.



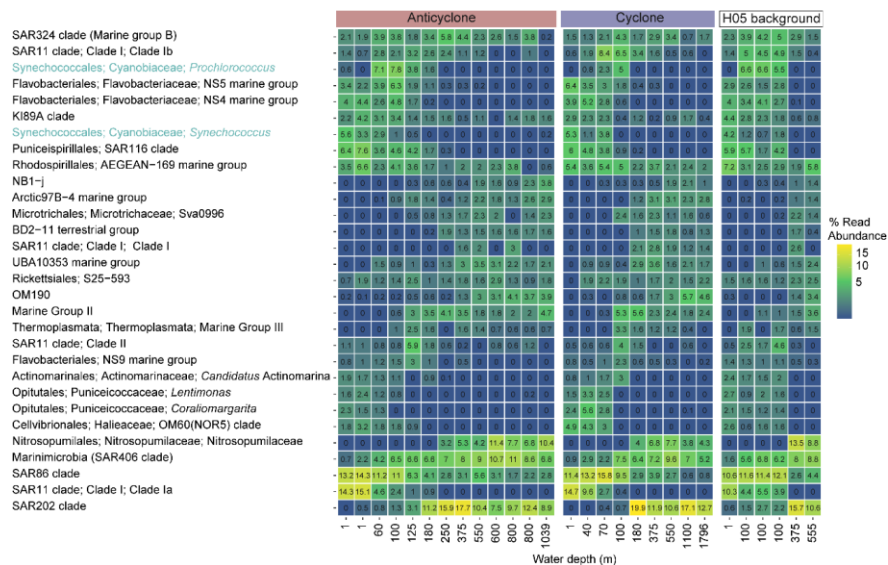


**Figure 4** – The relative abundance of 30 most-abundant bacterial and archaeal genera collected at cyclonic and anti-cyclonic eddies, and an uninfluenced background station at the southeastern Mediterranean Sea during October 2018, as estimated by read abundance. Results of replicate casts in anti-cyclone and uninfluenced background (H05) stations are shown in columns with identical depths.

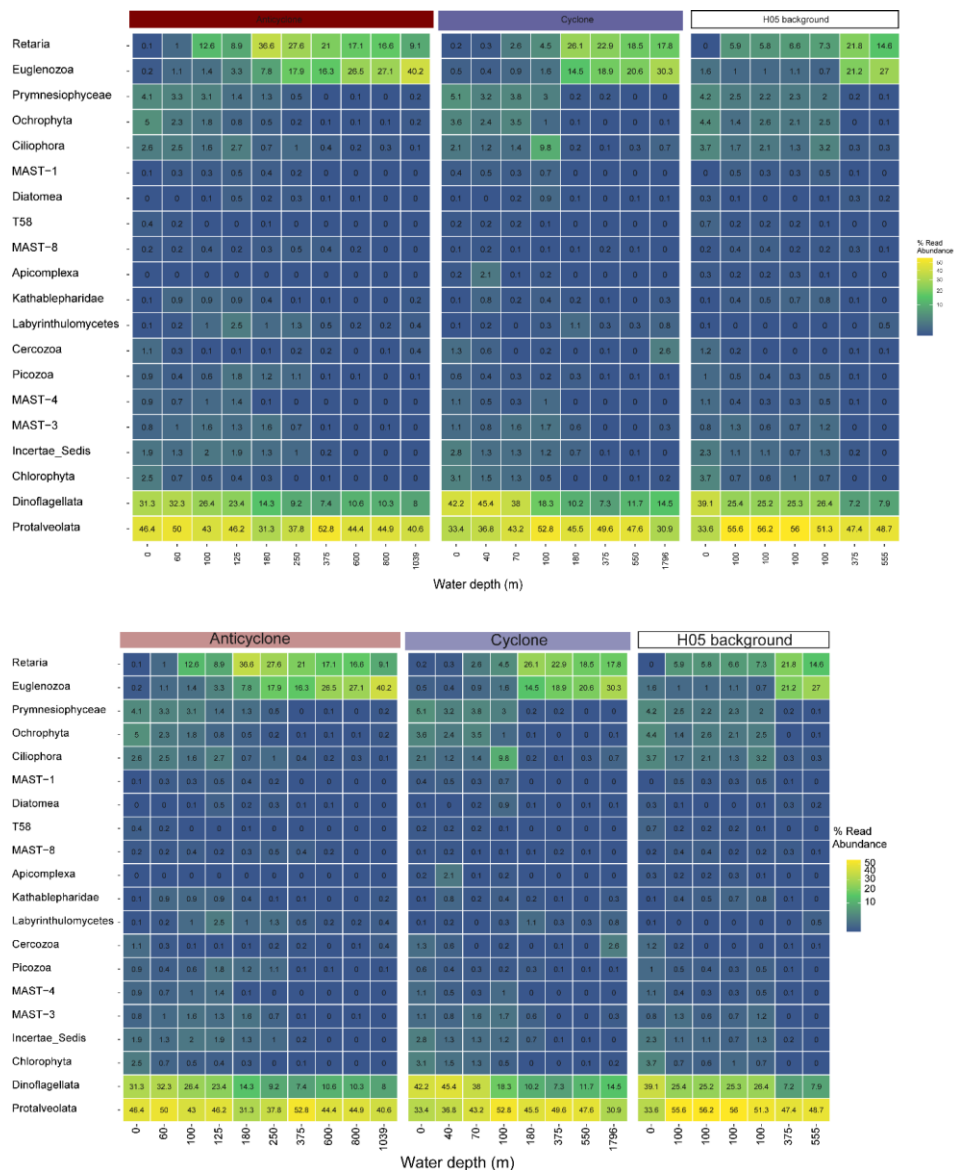


**Figure 5** – The relative abundance of 20 most-abundant unicellular eukaryotic lineages (phylum level), collected at cyclonic and anti-cyclonic eddies, and at an uninfluenced

background station (H05) at the southeastern Mediterranean Sea during October 2018, as estimated by read abundance. Results of replicate casts in anti-cyclone and control H05 stations are shown.

415 Following the higher nutrients levels and pico-phytoplankton biomass, PP was highest in the cyclone ( $191 \text{ mg C m}^{-2} \text{ d}^{-1}$ ) and significantly decreased by 50-80% at the background ( $81 \text{ mg C m}^{-2} \text{ d}^{-1}$ ) and anti-cyclone ( $36 \text{ mg C m}^{-2} \text{ d}^{-1}$ ) stations (**Tables 1, S1**). The highest PP rates were found in the surface water of all stations ( $\sim 0.8\text{-}2.0 \text{ } \mu\text{g C L}^{-1} \text{ d}^{-1}$ ) and decreased with depth throughout the photic layer (**Figure 3F**). The differences in the vertical distribution of chl-*a* and PP were also evident in the assimilation number of phytoplankton, which signifies autotrophic specific activity (PP per chl-*a*). The assimilation number was highest at the cyclone ( $10 \text{ g C g Chl-}a^{-1} \text{ d}^{-1}$ ) and lower by 60-80% in the anti-cyclone and background stations ( $2\text{-}4 \text{ g C g Chl-}a^{-1} \text{ d}^{-1}$ ) (**Tables 1, S1**). Integrated doubling times of pico/nano-phytoplankton was highest at the anti-cyclone (9.7 days) and lowest in the cyclone (3.1 days) (**Table 1**).

430 Total BA was higher by 1-2 orders of magnitude than the pico-phytoplankton abundance (**Figure 6A, Table S1**). The highest BA was measured at the anti-cyclone ( $2125 \times 10^{10} \text{ cells m}^{-2}$ ) followed by the cyclonic eddy ( $2072 \times 10^{10} \text{ cells m}^{-2}$ ) and background ( $1459 \times 10^{10} \text{ cells m}^{-2}$ ) stations (**Table 1**). Contrary to the BA or biomass, BP was significantly higher at the cyclone ( $214 \text{ mg C m}^{-2} \text{ d}^{-1}$ ) compared to the anti-cyclone and background stations ( $82\text{-}85 \text{ mg C m}^{-2} \text{ d}^{-1}$ ) (**Table 1**). A similar trend was measured in heterotrophic bacteria cell-specific activity (BP/BA), where the most productive cells were found at the cyclone ( $10 \text{ fg C cell}^{-1} \text{ d}^{-1}$ ), while the least productive cells were found at the anti-cyclone ( $4 \text{ fg C cell}^{-1} \text{ d}^{-1}$ ) (**Tables 1, S1**). Overall, BP was homogeneously distributed throughout the photic layer in all stations ( $\sim 0.2\text{-}0.9 \text{ } \mu\text{g C L}^{-1} \text{ d}^{-1}$ ), except the cyclonic eddy where the rates were relatively high in the upper 100 m ( $\sim 0.8\text{-}2.4 \text{ } \mu\text{g C L}^{-1} \text{ d}^{-1}$ ) (**Figure 6B**). At 180 m, BP rates were similar at all stations ( $\sim 0.1 \text{ } \mu\text{g C L}^{-1} \text{ d}^{-1}$ ) (**Figure 6B**). The resulting BP/PP ratio was overall similar outside the cyclone;  $\sim 1$ , and was twofold higher inside it (**Table 1**). In accordance with the high BP, the integrated doubling time of

heterotrophic bacteria was highest at the anti-cyclone (3.5 days) and lowest at the cyclone (1.4 days) (**Table 1**).

The slope of the log-log linear regressions for BA and BP obtained in the cyclonic eddy was 0.24 ( $R^2=0.60$ ), while in the anti-cyclonic eddy the slope was more than twice as high; 0.52 ( $R^2=0.79$ ) ( $P=0.03$ , Analysis of the Covariance [ANCOVA], Andrade & Estévez-Pérez 2014).

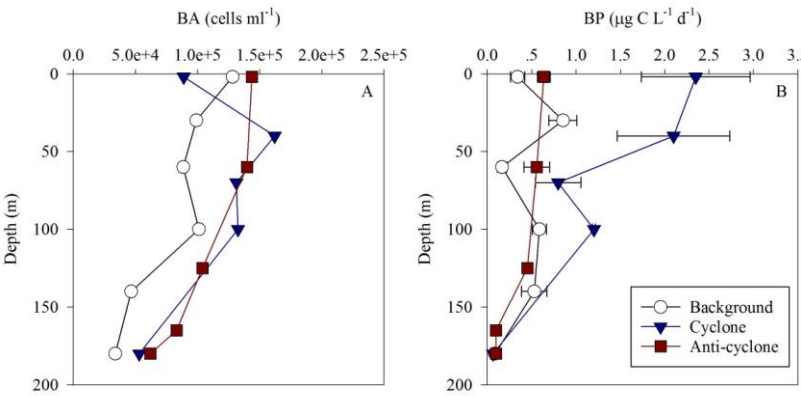


**Figure 6** – Vertical profile of heterotrophic bacterial abundance (A) and bacterial production rates (B) at the photic layer of cyclonic (blue triangle) and anti-cyclonic (red square) eddies and an uninfluenced background station (white circle) at the southeastern Mediterranean Sea during October 2018.

In accordance with the high PP and BP, total zooplankton biomass in the upper 300 m was an order of magnitude higher in the cyclonic eddy (3045 mg DW m<sup>-2</sup>, 1337 mg C m<sup>-2</sup>) compared with the anti-cyclonic (303 mg DW m<sup>-2</sup>, 133 mg C m<sup>-2</sup>) or background (360 mg DW m<sup>-2</sup>, 112 mg C m<sup>-2</sup>) stations (**Tables 1, S1**). Zooplankton grazing impact on phytoplankton stock estimates shows that meso-zooplankton consumed 30-38% of the daily phytoplankton stock in the anti-cyclone and background stations and 224% in the cyclone (Table 1). Similarly to zooplankton biomass, the estimated zooplankton carbon demand (ZCD) was highest in the cyclonic eddy (~388 mg C m<sup>-2</sup> d<sup>-1</sup>) and decreased by an order of magnitude in the anti-cyclonic eddy (~42 mg C m<sup>-2</sup> d<sup>-1</sup>) and the background (~34

mg C m<sup>-2</sup> d<sup>-1</sup>) stations (**Tables 1, S1**). Considering phytoplankton as the major food source, zooplankton potentially consumed 203% of PP in the cyclonic eddy, 116% in the anti-cyclonic eddy, and only 42% in the background station (**Tables 1, S1**). Zooplankton respiration rates were 9-11-fold larger in the cyclone (~166 mg C m<sup>-2</sup> d<sup>-1</sup>) than in the anti-cyclone and background stations (~15-19 mg C m<sup>-2</sup> d<sup>-1</sup>), corresponding to 87% vs. 18-53% of the integrated PP (**Tables 1, S1**). The estimated contribution of zooplankton to nitrogen regeneration by excretion of ammonium was 9-11 fold greater in the cyclone (25 mg N-NH<sub>4</sub> m<sup>-2</sup> d<sup>-1</sup>) than in the anti-cyclone or the background stations (~2-3 mg N-NH<sub>4</sub> m<sup>-2</sup> d<sup>-1</sup>), corresponding to 61% vs. 13-37% of the integrated PP (based on a C:N 5.4:1 ratio, Pujo-Pay et al., 2011) for the Levantine Basin water (**Tables 1, S1**). The estimated contribution of zooplankton to phosphorus (as orthophosphate) by excretion was an order of magnitude greater in the cyclone (3.6 mg P-PO<sub>4</sub> m<sup>-2</sup> d<sup>-1</sup>) than in the anti-cyclone and background stations (0.3-0.4 mg P-PO<sub>4</sub> m<sup>-2</sup> d<sup>-1</sup>), corresponding to 85% vs. 17-50% of the integrated PP (based on a C:P 116:1 ratio, Pujo-Pay et al., 2011) (**Tables 1, S1**).

Zooplankton alpha diversity estimated based on the COI and 18S rDNA genes read abundance as well as by cell abundance (i.e., microscopic identification) was highest in the cyclone and background stations, and lowest in the anti-cyclone (**Figure 7**). COI and 18S ASV richness (ACE index) were lowest in the anti-cyclone (29 and 81, respectively), and 60% (18S) to 250% (COI) larger in the cyclone and background stations (**Figure 7**). The lowest zooplankton biodiversity (Shannon and Simpson indices) was found in the anti-cyclone, using both genes (**Figure 7**). These findings were confirmed with rarefaction curves (**Figures S8, S9**).



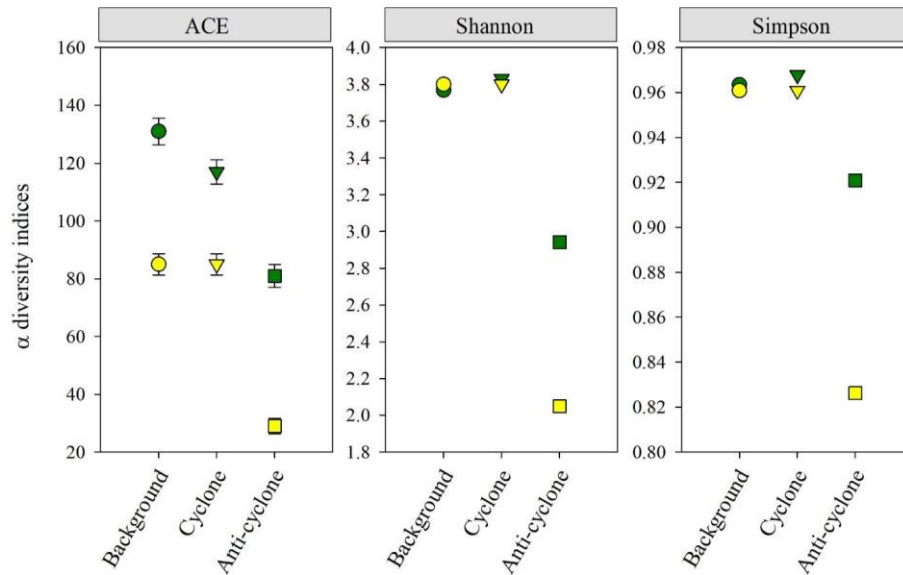


**Figure 7** – Zooplankton alpha diversity indices (ACE  $\pm$ SE, Shannon, Simpson) based on 18S (green) and COI (yellow) amplicon sequencing in >100- $\mu$ m samples collected from the upper 300 m of cyclonic and anti-cyclonic eddies, and at an uninfluenced background station at the southeastern Mediterranean Sea during October 2018.

Classification to species level was successful in 211 out of 221 COI ASVs and in only 55 out of 830 18S ASVs, 200 of which were classified to an order level. The three stations differed in the zooplankton relative richness (i.e., number of ASVs per taxonomical functional group) (**Figure 8**). Overall, in all stations, copepods (Hexanauplia) were the most diverse group, nevertheless, copepod richness was 7-fold larger in the cyclone vs. the anti-cyclone. Ostracods and hydrozoans (mainly siphonophores) had higher diversity in the background station than in the other stations. Chaetognaths, branchiopods (cladocerans), planktonic decapods and amphipods, had similar richness levels in the cyclonic eddy and background stations, however, they were completely absent in the anti-cyclone. In contrast, a higher richness of gastropods (mainly pteropods) was found in the anti-cyclone compared

to the cyclone and background stations. Although the majority of the taxonomic groups were better represented by COI classification, one group – Polychaeta – was better represented in the 18S rRNA (2 versus 12 ASVs), as 18S is more often used to obtain resolved phylogenies in polychaetes (Colgan et al., 2006). Based on the 18S rRNA gene ASVs, the highest richness of polychaetes was found in the cyclone (6 ASVs) and background (5 ASVs) stations, whereas only 2 ASVs were found in the anti-cyclone.

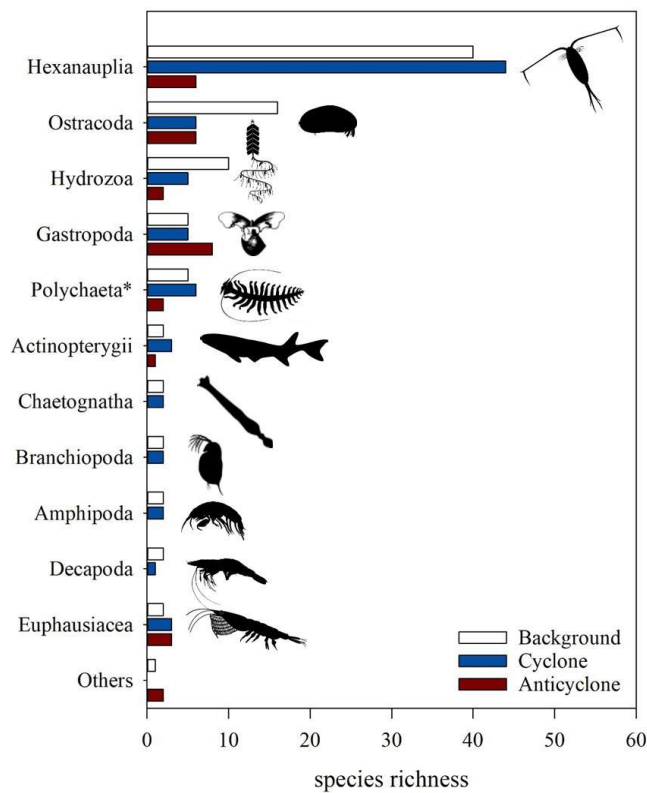


**Figure 8** – Zooplankton species richness based on COI amplicon sequences (classified using BOLD/NCBI-based database) in >100-μm samples collected from the upper 300 m of cyclonic and anti-cyclonic eddies, and at an uninfluenced background station at the

southeastern Mediterranean Sea during October 2018. \*Polychaeta richness was obtained  
 510 from rRNA 18S amplicon sequences.

**Table 1** – Chemical and biological integrated values at the upper 180 m (except  
 zooplankton where 0-300 m is presented) measured in the different sampling sites. The  
 515 maximal values for each variable are highlighted in bold.

Variable	Background	Cyclone	Anti-cyclone
NO <sub>x</sub> (mmol m <sup>-2</sup> )	35.5	<b>121.2</b>	9
PO <sub>4</sub> <sup>3+</sup> (mmol m <sup>-2</sup> )	2.4	<b>2.5</b>	1
N:P	15	<b>48</b>	9
Si(OH) <sub>4</sub> (mmol m <sup>-2</sup> )	150.2	<b>200.7</b>	133.3
Chl- <i>a</i> (mg m <sup>-2</sup> )	<b>21.3</b>	20	17.9
<i>Synechococcus</i> (x10 <sup>10</sup> cells m <sup>-2</sup> )	<b>69</b>	27	54
<i>Prochlorococcus</i> (x10 <sup>10</sup> cells m <sup>-2</sup> )	231	163	<b>273</b>
Pico-eukaryotes (x10 <sup>10</sup> cells m <sup>-2</sup> )	1.7	<b>7.2</b>	2.3
Nano-eukaryotes (x10 <sup>10</sup> cells m <sup>-2</sup> )	3.3	<b>6.3</b>	3
Total pico/nano-phytoplankton biomass (mg C m <sup>-2</sup> )	369	<b>597</b>	348
Heterotrophic bacteria (x10 <sup>10</sup> cells m <sup>-2</sup> )	1459	2072	<b>2125</b>
Heterotrophic bacteria biomass (mg C m <sup>-2</sup> )	204	290	<b>298</b>
Zooplankton biomass (mg DW m <sup>-2</sup> )	360	<b>3045</b>	303
Zooplankton biomass (mg C m <sup>-2</sup> )	112	<b>1337</b>	133
Grazing impact on phytoplankton stock (%)	30	<b>224</b>	38
PP (mg C m <sup>-2</sup> d <sup>-1</sup> )	81	<b>191</b>	36
AN (g C g Chl- <i>a</i> <sup>-1</sup> d <sup>-1</sup> )	4	<b>10</b>	2
Phytoplankton doubling time (d)	4.6	3.1	<b>9.7</b>
BP (mg C m <sup>-2</sup> d <sup>-1</sup> )	82	<b>214</b>	85
Heterotrophic bacteria doubling time (d)	2.5	1.4	<b>3.5</b>
BP/BA (fg C cell <sup>-1</sup> d <sup>-1</sup> )	5.7	<b>10.3</b>	4.0
BP/PP	1.0	1.1	<b>2.4</b>

Zooplankton carbon demand (mg C m <sup>-2</sup> d <sup>-1</sup> )	34.3	<b>387.9</b>	41.8
Grazing impact on PP (%)	42	<b>203</b>	116
Zooplankton respiration (mg C m <sup>-2</sup> d <sup>-1</sup> )	14.8	<b>166.2</b>	18.9
% of PP respired by zooplankton	18	<b>87</b>	53
Zooplankton excretion (mg N-NH <sub>4</sub> m <sup>-2</sup> d <sup>-1</sup> )	2.2	<b>25</b>	2.9
Phytoplankton N demand (mg N m <sup>-2</sup> d <sup>-1</sup> )	17	<b>41</b>	8
% contribution of zooplankton N to PP	13	<b>61</b>	37
Zooplankton excretion (mg P-PO <sub>4</sub> m <sup>-2</sup> d <sup>-1</sup> )	0.3	<b>3.6</b>	0.4
Phytoplankton P demand (mg P m <sup>-2</sup> d <sup>-1</sup> )	1.8	<b>4.2</b>	0.8
% contribution of zooplankton P to PP	17	<b>85</b>	50

#### 4 Discussion

Seasonality is the primary driver affecting water column characteristics in the SEMS, where external inputs of nutrients such as from the atmosphere (Herut et al., 2002, 2005; Ridame et al., 2011) or large rivers (Krom et al., 2014; Ludwig et al., 2009) are limited in space and time. Thus, the one-dimensional processes of summer stratification and winter mixing determine, to a large extent, the nutrient availability in the photic layer (<180 m), subsequently affecting phytoplankton population dynamics and activity (van Ruth et al., 2020). However, horizontal variability plays an important role. Turbulent mesoscale eddies are a prominent part of the circulation in the SEMS (Mkhinini et al., 2014). Such features have lifetimes of a few months to a year (Mkhinini et al., 2014), affecting the availability of the nutrients to phytoplankton and bacteria in the photic layer (Rahav et al., 2013; Vaillancourt et al., 2003), and thus to higher trophic levels (Dolan et al., 2002; Siokou-Frangou, 2004). The degree to which an eddy affects the community depends on the eddy's size, age, the source of the water 'trapped' within it, and the interaction with wind and land (Gaube et al., 2014; Huggett, 2014; Landry et al., 2008; Strzelecki et al., 2007). Our results demonstrate that upwelling within the cyclone injected deeper water nutrients into the quasi-permanent eddy, thus fertilizing the planktonic population.

The effect of hydrodynamic structures on planktonic microbial distribution has been studied previously in the SEMS. However, these studies focused on long-lived anti-

cyclonic eddies such as the Cyprus/Shikmona Eddy (>6 months, Christaki et al., 2011; Rahav et al., 2013; Thingstad et al., 2005). There is a strong asymmetry in eddy's lifetime, which on average is far shorter for cyclones than anti-cyclones. This asymmetry is enhanced in the SEMS where the cyclone lifetime distribution is very similar to the rest of the Mediterranean Sea, yet the anti-cyclones live longer (Mkhinini et al., 2014). It makes the comparison of cyclones and anti-cyclones more challenging in the SEMS as they are not circulating (and thus isolated) for the same time. We sampled a recent anti-cyclone (#12683, two months old) and a more 'mature' cyclone (#11988, over a year old), which is not the usual scenario in the SEMS. The short-lived anti-cyclone and the background station indeed have similar characteristics. We expect long-lived anticyclones to be even more oligotrophic, making their influence more prominent, as discussed below.

#### 4.1. Pico-phytoplankton dynamics and primary production in anti-cyclonic and cyclonic waters

Our results show that nutrient availability affected the pico-phytoplankton dynamics in the SEMS. The low pico-eukaryotes biomass and the low N:P in the anti-cyclonic eddy (~9:1) suggest N limitation for these autotrophs under extreme oligotrophic conditions (**Table 1**). Contrary, the high N:P ratio (~48:1) and the relatively low cyanobacterial biomass in the cyclonic eddy suggest that *Synechococcus* and *Prochlorococcus* are P-limited. These results are similar to a previous study from the SEMS showing that NO<sub>x</sub> concentrations at the Rhodes Gyre (up-welling) were 5-fold higher than in the Cyprus Eddy (down-welling), while PO<sub>4</sub><sup>3+</sup> remained similarly low for the two locations (Rahav et al., 2013). These variations result in significant differences in the NO<sub>x</sub>:PO<sub>4</sub><sup>3+</sup> ratio of the two systems; Rhodes Gyre (~ 50:1) and Cyprus Eddy (~10:1), implying similar nutrient limitations as discussed above. Stoichiometric N:P Redfield ratio alone, however, cannot fully explain which nutrients limit the microbial plankton diversity. Some phytoplankton species have nutritional requirements different than N:P=16, and there are several 'non-Redfield' processes in the aquatic ecosystem, which may alter the N:P ratio, regardless of any nutrient limitation (Arrigo, 2005; Geider and La Roche, 2002; Moore et al., 2013).

The integrated chl-*a* content at the background, the anti-cyclone, and the cyclonic stations exhibited overall low variability (~18-21 mg chl-*a* m<sup>-2</sup>), yet the integrated primary

production in the cyclone was ~5 times higher, resulting in a higher assimilation number. This high assimilation number indicates a better efficiency of carbon incorporation per chl-*a* unit and thus a better algal physiological state at the cyclone relative to that of other stations considered. This is likely owing to the higher nutrient availability (i.e., N and P) at the cyclone relative to the other more oligotrophic sites sampled (**Table 1**). It may also suggest different community compositions and cell sizes.

The overall low PP outside the cyclone (**Figure 3F**, **Table 1**) is in accordance with another low nutrient low chl-*a* (LNLC) systems (Falkowski et al., 2003; Lomas et al., 2013) and aligned with the threshold limit of oligotrophic oceans;  $< 100 \text{ mg C m}^{-2} \text{ d}^{-1}$  (Koblentz-Mishke et al., 1970). Low PP may be driven by several factors such as nutrient availability (Kress et al., 2005), light levels (Dishon et al., 2012; Sathyendranath and Platt, 2007; Stambler, 2012), viral infection (Guixa-Boixereu et al., 1999b, 1999a), and top-down grazing by zooplankton (Griffin and Rippingale, 2001; Olli et al., 2007; Rakhesh et al., 2008). We surmise that the overall low PP was mainly driven by the N and P standing stocks in the photic layer, including the cyclone (**Table 1**). This is because light levels were similar in all stations and therefore unlikely to affect the daily PP rates between sites. Moreover, viral-induced mortality was shown to be less important than mortality due to grazing by protists in the SEMS as has been shown in unamended eastern Mediterranean surface water in mesocosms (Tsiola et al., 2017). Contrary, the grazing impact on phytoplankton was significantly higher in the cyclone compared to the other more oligotrophic sites (~200% vs. ~40-100%, respectively, **Table 1**). Despite the potentially high grazing pressure in the cyclone, higher phytoplankton biomass and PP were measured in this upwelling site. These differences between sites are likely attributed to the different phytoplankton growth rates, as phytoplankton's doubling time at the cyclone was ~3 days, while 5-10 days was estimated in the anti-cyclone and background stations. These doubling time estimates are in the same order as reported in other marine environments, ranging from ~1 day (reviewed in Laws 2013) to 10 days (Dyhrman et al., 2012), and are in agreement with recent estimates from the central and western Mediterranean Sea (Marañón et al., 2021). We note that doubling time estimates have many caveats, mostly because some phytoplankton or bacteria comprise an unknown fraction of the POC pool, and it is a methodological challenge to separate them from all other particles in the water (Laws,

2013). Moreover, grazing impact on PP calculated from mesozooplankton biomass alone  
 600 may lead to an overestimation of the top-down impact on autotrophic microbial populations  
 (Feliú et al., 2020). Therefore, it is likely that we overestimated the grazing impacts on PP,  
 which exceeded 100% in the cyclone (**Table 1**). Some mesozooplankton species can  
 simultaneously graze both phytoplankton and heterotrophic prey (i.e., heterotrophic  
 dinoflagellates and ciliates, Dolan et al., 2002; Sherr and Sherr, 2007). Such a  
 605 “multivorous” feeding strategy may explain the >100% mesozooplankton grazing impact  
 on PP in the cyclone (Gasol et al., 1997). Moreover, the high estimated contribution of N  
 and P by zooplankton to the PP by excretion at the cyclone (61-85%, **Table 1**) suggests  
 rapid nutrient recycling that fuels the high production at this site. Contrary, in the anti-  
 cyclone and background stations a lower N and P excretion by zooplankton was estimated  
 610 (**Table 1**), therefore support only a minor part of the PP.

#### **4.2 Heterotrophic bacterial abundance and production in anti-cyclonic and cyclonic waters of the SEMS**

Prokaryotic microorganisms are important components of the marine food web,  
 615 playing a pivotal role in many biogeochemical cycles (e.g., Kirchman, 2012). In warm and  
 oligotrophic environments, such as the SEMS, heterotrophic bacterial metabolism is often  
 equal or even higher than autotrophic activity (Luna et al., 2012; Pulido-Villena et al.,  
 2012; Rahav et al., 2019). Our results show that while the abundance of heterotrophs was  
 overall similar in the cyclone and anti-cyclone, their cell-specific activity was nearly  
 620 threefold higher in the nutrient-rich cyclone (**Table 1**). Given that average bacteria  
 contain 14 fg C cell<sup>-1</sup> (Gundersen et al., 2002), our estimate of bacterial cell-specific  
 activity suggests that heterotroph doubling time in the cyclone is ~2 faster than the less  
 productive anticyclone and background stations (**Table 1**). The differences in cell-specific  
 activity and corresponding doubling time between sites are likely supported by the  
 625 supplement of limiting nutrients for heterotrophic bacteria. Previous studies showed that P  
 and/or dissolved organic carbon (DOC) are the limiting factors for heterotrophic microbial  
 activity in the SEMS (Pitta et al., 2017; Rahav et al., 2019, 2021). We hypothesize that in  
 the cyclone heterotrophic bacteria are likely DOC rather than P-limited since the PO<sub>4</sub><sup>3+</sup>  
 concentrations at this location were ~3-fold higher than in the other locations (**Table 1**).

630 The high mesozooplankton excretion in the cyclone may add DOC and inorganic nutrients,  
which could partly fulfill the metabolic requirements of the heterotrophic bacteria.  
Contrary, in the background and anti-cyclone stations heterotrophic prokaryotes were  
likely P limited, as previously demonstrated in onboard microcosm experiments (Rahav et  
al., 2021; Zohary et al., 2005) and using indirect N:P stoichiometric mass balance  
635 calculations (Krom et al., 2005).

The ratio between BP and PP is commonly used as an indicator for the carbon flux  
derived from photosynthesis channeled through the microbial heterotrophic food web  
(Cole et al., 1988). The higher the ratio, the lower the amount of carbon available for export  
through herbivorous food webs. Here, the BP rates were two times higher than PP in the  
640 LNLC anti-cyclone (**Table 1**), suggesting that microbial heterotrophs outcompeted  
phytoplankton for most of the available nutrients. The equal BP and PP in the background  
and the cyclone stations demonstrate an imbalanced microbial metabolism, highlighting  
the importance of heterotrophy in SEMS. Previous studies from the anti-cyclonic Cyprus  
Eddy (Thingstad et al., 2005) and throughout the Mediterranean Sea (Rahav et al., 2021)  
645 suggested that heterotrophic bacteria may outcompete phytoplankton or diazotrophs for  
 $\text{PO}_4^{3-}$ . This is in contrast to most oceanic regimes, in which  $\text{BP:PP} < 1$  at the photic layer  
(e.g., Lomas et al., 2013). We note that some studies suggest that a net heterotrophy in a  
given system is biased due to an underestimate of PP and/or an overestimate of respiration  
rate. We currently cannot refute nor reinforce this debate, as we did not measure respiration  
650 rates. Community respiration rate measurements, although technically challenging, are  
needed, especially in light of the future climate-change predictions stating the oceans will  
become more heterotrophic (Duarte et al., 2013).

The slope of the log-log linear regressions for BA (as a biomass) and BP (a proxy  
of resource availability) suggest that bacterioplankton were bottom-up regulated in the  
655 anti-cyclone and top-down regulated in the cyclone (Billen et al., 1990; Ducklow, 1992;  
Pulido-Villena et al., 2012), in agreement with the estimated growth rates calculated above  
(sub-section 4.2). These values concur with other studies from the Mediterranean offshore  
water where the log-log regression of BA vs. BP is usually  $\sim 0.40$  (Ducklow, 1992; Mével  
et al., 2008; Zohary and Robarts, 1998). Top-down and bottom-up factors are constantly  
660 changing in oligotrophic environments where organic matter flux is sporadic rather than



continuous and where PP and grazing pressure may vary greatly on a temporal scale (Pulido-Villena et al., 2012). Understanding the feedback mechanisms controlling heterotrophic bacterial abundance and production in LNLC environments is of great ecological importance, especially in areas such as the Mediterranean Sea where the water column is rapidly warming and thus heterotrophic metabolism is likely to be more dominant (Luna et al., 2012; Rahav et al., 2019).

#### 4.3 Zooplankton biomass, estimated carbon and nutrient demand

Our results show that zooplankton biomass was one order of magnitude higher in the more productive cyclone than in the anti-cyclone and background stations. This is in line with previous studies (Goldthwait and Steinberg, 2008; Landry et al., 2008b; Liu et al., 2020; Riandey et al., 2005; including the Levantine Basin Mazzocchi et al., 1997; Pancucci-Papadopoulou et al., 1992), which showed that higher productivity (either as PP or chl-*a* levels) in cyclonic eddies leads to higher zooplankton biomass. Zooplankton biomass reflected the higher PP at the photic layer, rather than the standing stock of the primary producers, possibly due to the higher estimated grazing impact on phytoplankton stock in the cyclone vs. the anti-cyclone and background stations (**Table 1**). A recent study from the central and western Mediterranean Sea demonstrated that the nutrient diffusive fluxes across the nutricline contribute only a minor fraction of the phytoplankton N and P requirements in the deep photic layer (Marañón et al., 2021). This suggests that generally phytoplankton depend on regenerated nutrients for growth rather than their supply from the nutricline in the SEMS.

The estimated integrated contribution of zooplankton to carbon turnover and nutrient remineralization was markedly higher in the cyclone than in the anti-cyclone and background stations. Since the dietary needs of some zooplanktonic species diverge from the Redfield ratio (Arrigo, 2005; Geider and La Roche, 2002; Moore et al., 2013), our estimates are based on the particulate C:N:P values reported from the Levantine basin water (Pujo-Pay et al., 2011). The contribution of  $\text{PO}_4^{3-}$  by excretion of zooplankton to the estimated demand of phytoplankton was higher than their contribution of N (~85% vs ~60% respectively). The fact that there is a markedly high excess of N relative to P in the photic layer of the cyclone (**Table 1**), implies that the P was consumed not only by phytoplankton. This further support the ‘orthophosphate bypass theory’ suggested by

Thingstad et al., (2005) which showed that  $\text{PO}_4^{3+}$  can be rapidly transferred through the microbial food web to copepods, bypassing the phytoplankton compartment, via luxury consumption mechanisms that shift the stoichiometric composition of copepod prey.

695 In addition to the higher PP rates, the higher zooplankton concentrations in the cyclone may also be attributed to lower temperatures, potentially providing a thermal refuge for different larvae as shown by model simulations (Limer et al., 2020). Such a temporal or quasi-permanent shelter from detrimental environmental conditions can be especially important to the native biota in the rapidly warming Levantine Basin (Ozer et al., 2017). Furthermore, the warmer waters of anti-cyclonic eddies, arriving from the  
700 southeastern corner of the Levantine basin (as in our case, **Figure S2**), may carry thermophilic Indo-Pacific species, and facilitate their introduction and spread throughout the SEMS. The potential role of cyclonic eddies as thermal refugia for native species and anti-cyclonic eddies as introduction and dispersal vector for alien Indo-Pacific species  
705 should be investigated in future studies as cyclonic and anti-cyclonic features are likely to become more prominent in the future Mediterranean Sea (Siokou-Frangou et al., 2010).

#### 4.4 Diversity of bacterioplankton and planktonic protists

Multivariate analyses of bacterioplankton diversity suggest that at the DCM and  
710 180 m depths, the bacterioplankton community at the cyclone station differed from that of the respective depths at the anti-cyclone and background stations (**Figure S10**). These changes may be attributed to the depths of the nutricline, which vary between locations (**Figure 2**), and/or selective grazing pressure caused by different zooplankton species with different nutrition preferences (see discussion below). The microbial communities at the  
715 cyclone station were more similar to those of the deeper depths at the anti-cyclone and background stations. For example, the DCM community of the cyclone resembled the community at 180 m depth of the anti-cyclone (**Figure S10**). It has been shown that nutrient-poor anti-cyclonic gyres select for *Prochlorococcus* (Vaillancourt et al., 2003), and potentially for diazotrophs (Church et al., 2009; Fong et al., 2008; Rahav et al., 2013).  
720 Alongside the integrated cell counts (**Table 1**), diversity analyses suggest that *Prochlorococcus* is indeed most abundant at the anti-cyclone (~8% read abundance at the DCM), as opposed to ~5-6% at the control and cyclone's DCM communities. We have,

however, not identified cyanobacterial diazotrophs such as *Trichodesmium* and UCYN-A in any of our stations, in agreement with previous findings that showed uncoupling of PP and N<sub>2</sub> fixations in the SEMS (Rahav et al., 2013). Apart from *Prochlorococcus*, ASVs of heterotrophic/mixotrophic lineages, such as SAR324, Flavobacteriales, Rhodospirillales, Punicespirillales, Oritales, SAR86, SAR11 were depleted at the cyclone's DCM (DESeq2, adjusted p<0.05), implying a community-level shift driven by up-welling and down-welling processes. The actual drivers of these shifts (e.g., water mass movement, temperature, nutrient availability, interactions with another biota including phage predation) remain to be elucidated.

High N:P ratios were suggested to have a large effect on the diversity of micro-eukaryotes (e.g., Cercozoa, Ciliophora and Dinoflagellata), while pico- and nanoeukaryotes (e.g., dinoflagellates, Bacillariophyta, Chlorophyta and Haptophyta) are more adapted to the P-poor (and thus high N:P) conditions due to their high surface to volume ratio (Kruk and Segura, 2012). In agreement with this notation, we found that the Oligotrichia ciliates (Ciliophora) comprised ~9% ASV read abundance in the cyclone DCM; opposed to <1% at the anti-cyclone/background stations. These ciliates can feed on algae (as well as bacteria) and retain ingested chloroplasts (McManus et al., 2018), and thus potentially contribute to PP. However, we also identified a high read abundance of Radiolaria (RAD A, Retaria) at the anti-cyclone's DCM (~9%, **Figure S5**), indicating either that these organisms were indeed abundant, or suggesting that radiolarians that often carry multiple nuclei (Suzuki et al., 2009) may introduce noise to the marker gene diversity results.

The potentially toxic dinoflagellate *Karlodinium* was most abundant at the anti-cyclone's DCM (2.1-2.6% of ASV reads) and least abundant at the cyclone station's DCM (0.7% of ASV reads). A previous study suggested that the presence of this dinoflagellate may be related to P limitation, where it can switch from autotrophy to phagotrophy to take up nutrients from prey (Lin et al., 2016), providing it a competitive advantage. Indeed, the very low levels of PO<sub>4</sub><sup>3+</sup> in the DCM of the anti-cyclone (below detection limit), opposed to the cyclone's DCM (~0.02 μmol Kg<sup>-1</sup>), may explain the presence of this dinoflagellate and highlight that the different nutrient regimes may alter the diversity of protist communities in the SEMS.

Temperature is the main factor governing the distribution of planktonic protists in the SEMS (Santi et al., 2020). It is thus likely that the marked differences in the surface water temperature affect the diversity patterns of protists in warm and cold-core eddies. In the anti-cyclone, Syndiniales, which includes several known parasitic microbes (Guillou et al., 2008) were markedly enriched in surface waters (12 Syndiniales ASVs) relative to the other stations sampled. The relative abundance of these dominant parasites, which infect and kill other protists, such as dinoflagellates, cercozoans and radiolarians, as well as metazoans (Clarke et al., 2019), positively correlates with temperature (Anderson and Harvey, 2020). This is likely because temperature accelerates their metabolic rates, increasing infectivity and dinospore production (Anderson and Harvey, 2020; Coats and Park, 2002).

#### 4.5 Zooplankton diversity in anti-cyclonic vs. cyclonic waters at the SEMS

Cyclonic and anti-cyclonic eddies can entrain different zooplankton communities and biodiversity, distinctly different in their biogeographic origin from the adjacent waters (Hernández-León et al., 2001; Isla et al., 2004; Mackas et al., 2005; Pinca and Dallot, 1995; Riandey et al., 2005). In our study, we used meta-barcoding of mitochondrial (COI) and nuclear (18S) genes to assess the diversity of the mesozooplankton communities in the background, cyclone and anti-cyclone stations. We found that, although the background station had zooplankton biomass similar to that of the anti-cyclone, its community had high richness and diversity, comparable with that of the cyclone. Different and contrasting diversity patterns have been previously recorded in cyclonic vs. anti-cyclonic eddies relative to the surrounding waters. This includes reports on a higher diversity in cyclonic eddies (Matis et al., 2014; Pinca and Dallot, 1995), lower diversity in cyclonic eddies (Lavaniegos and Hereu, 2009), higher diversity in anti-cyclonic eddies (Dufois et al., 2016), and lower diversity in anti-cyclonic eddies as found in the majority of the studies (Holliday et al., 2011; Isari et al., 2011; Liu et al., 2020; Matis et al., 2014; Pinca and Dallot, 1997; Seguin et al., 1994). These contradicting patterns of diversity might be related to the difference in ages of the respective mesoscale features, as found in our case, or be related to the initial chemical characteristics of the respective environment (i.e., oligotrophic, mesotrophic or eutrophic). Low nutrient levels, as were measured in the anti-cyclone (Table 1), can promote the inter-specific competition on resources, favoring some

785 species at the expense of others, thus decreasing species richness and evenness (Pinca and  
Dallot, 1997; Pitta et al., 2016; Seguin et al., 1994; Thingstad et al., 2005).

Copepods generally dominate mesozooplankton assemblages, both in terms of  
abundance and biomass and are important in the transfer of oceanic carbon, and as a food  
source for higher trophic levels (Frangoulis et al., 2004). Because they are trophically  
790 diverse, the richness and diversity of copepods can reflect major changes in underlying  
patterns of production in the upper water column (Bonnet and Frid, 2004). In this study,  
copepod diversity presented a markedly large difference between the species-rich cyclone  
(44 species) and the species-poor anti-cyclone (6 species). Most of the copepod species in  
the anti-cyclone were small-body calanoids, e.g., *Clausocalanus* and *Calocalanus* species.  
795 Medium and larger size calanoid copepods, such as *Pleuromamma*, *Euchirella*,  
*Scolecithricella*, *Ctenocalanus*, *Nannocalanus* and *Mesocalanus* were only present in the  
cyclone and background stations. Similar diversity patterns were observed in the Liguro-  
Provençal Basin, cyclonic and anti-cyclonic gyres in the Ionian and Levantine seas and the  
Black Sea (Pinca and Dallot, 1997; Siokou-Frangou et al., 1997). In contrast to calanoid  
800 copepods, the *Oncaea* species were present only in the cyclone; these cruising detritivores  
likely benefit from the relatively higher phytoplankton biomass and productivity (**Figure  
3 and Table 1**).

Cyclonic structures have been associated with favorable habitats for reproduction  
and larval recruitment of many fish species, entraining higher larval abundance and  
805 diversity (Bakun, 2010; Condie and Condie, 2016; Logerwell and Smith, 2001; Matis et  
al., 2014; Mullaney and Suthers, 2013). In this study, we found a higher diversity of fish  
larvae and eggs in the cyclone, mainly including *Engraulis encrasicolus* (the European  
anchovy). Up-welling regions in the Alboran Sea, the Gulf of Lion and the nearby Catalan  
Sea, the Adriatic Sea and the North Aegean Sea are known as successful spawning grounds  
810 and areas of high productivity of small pelagic fish, mainly anchovy and sardine (Agostini  
and Bakun, 2002; Palomera et al., 2007; Stergiou et al., 1997). In the impoverished SEMS,  
the importance of cyclonic eddies as “high productivity islands” for fish reproduction and  
recruitment might be high. Indeed, our finding suggests that cyclonic eddies may serve as  
reproduction hotspots and nursery grounds of anchovies.

815 Other taxonomic groups, specifically chaetognaths, polychaetes, cladocerans and  
pelagic amphipods and decapods, exhibited higher richness in the cyclone compared to the  
anti-cyclone. An exception to the higher species diversity within the cyclone was the  
gastropods that showed higher diversity in the anti-cyclone station. A potential reason  
could be the thermophilic nature of many of the taxa identified in the anti-cyclone,  
820 including the larvae of a Red-Sea Lessepsian invader, *Nerita sanguinolenta*. An adult  
individual of this species was recently recorded on the Israeli Mediterranean coast for the  
first time (Rabi et al., 2020). Mesoscale and sub-mesoscale structures can promote  
introductions of invasive species or recruitment of harmful species, such as the destructive  
crown-of-thorn starfish (Miller et al., 2015), the extremely venomous box jellyfish  
825 *Irukandji* (Gershwin et al., 2013), and a sea urchin overgrazing the kelp forests (Ling and  
Johnson, 2009). In the SEMS, anti-cyclonic eddies originate from the alongshore current  
in the southeastern corner of the basin, in the vicinity of the Suez Canal opening. We can  
therefore hypothesize that the higher temperatures in anti-cyclonic eddies and their  
southeastern origin, might facilitate the introduction and spread of the warm-adapted  
830 invasive Red-Sea species. This finding has important implications for conservation and  
management and should be followed by additional research to substantiate the connection  
between Lessepsian invasive species and hydrodynamic structures in the Mediterranean  
Sea. Moreover, more studies of mesoscale features through their lifetime are required to  
improve the predictions of future conditions and to model the productivity of the  
835 Mediterranean Sea and other LNLC regims in light of global climate changes and the need  
to reduce the atmospheric carbon print.

#### Author contributions

840 Conceptualization; N.B, T.G-H, M.R-B, A.L, B.H and E.R; Data curation; I.G, T.O, T.G-  
H, A.L; Formal analysis; N.B, T.G-H, M.R-B, R.K, A.R. M, G.S-V, A.L, J.S and E.R;  
Project administration; A.L, G.S-V; Writing original draft; N.B, T.G-H, R.K, M.R-B,  
A.L, I.G, T.O, B.H and E.R.

#### Competing interests

None.

Formatted: Normal, Justified, Indent: First line: 1.27 cm,  
After: 0.01 cm

845 **Special issue statement**

The article is part of the special issue “Advances in interdisciplinary studies at multiple scales in the Mediterranean Sea”.

**Acknowledgments**

We would like to thank the R.V. *Bat-Galim* captains and crew for help at sea. The authors  
850 also thank Briac Le Vu, Evangelos Moschos and Alexandre Stegner for producing the  
AMEDA map, and François Carlotti and Marc Pagano for their help with zooplankton rate  
calculations. This work was partly supported by the National Monitoring Program of  
Israel's Mediterranean waters and by The Israel Science Foundation (grant # 1666/18 to  
A.L.) and by the Ministry of Science and Technology (MOST) (grant # 3-17933 to T.G-  
855 H.). RK was supported by the Deutsche Forschungsgemeinschaft as part of the  
Sonderforschungsbereich 754 ‘Climate–Biogeochemistry Interactions in the Tropical  
Ocean’ and by a Make Our Planet Great Again grant of the French Agence Nationale de la  
Recherche under the ‘Programme d’Investissements d’Avenir’, reference ANR-19-  
MPGA-0012.

860 **References**

- Agostini, V. N. and Bakun, A.: “Ocean triads” in the Mediterranean Sea: Physical  
mechanisms potentially structuring reproductive habitat suitability (with example  
application to European anchovy, *Engraulis encrasicolus*), *Fish. Oceanogr.*, 11(3), 129–  
142, doi:10.1046/j.1365-2419.2002.00201.x, 2002.
- 865 Alcaraz, M., Calbet, A., Estrada, M., Marrasé, C., Saiz, E. and Trepát, I.: Physical control  
of zooplankton communities in the Catalan Sea, *Prog. Oceanogr.*, 74(2–3), 294–312,  
doi:10.1016/j.pocean.2007.04.003, 2007.
- Allen, C. B., Kanda, J. and Laws, E. A.: New production and photosynthetic rates within  
and outside a cyclonic mesoscale eddy in the North Pacific subtropical gyre, *Deep. Res.*  
870 I, 43, 917–936, doi.org/10.1016/0967-0637(96)00022-2, 1996.
- Amaral-Zettler, L. A., McCliment, E. A., Ducklow, H. W. and Huse, S. M.: A method for  
studying protistan diversity using massively parallel sequencing of V9 hypervariable  
regions of small-subunit ribosomal RNA Genes, *PLoS One*, 4(7), 1–9,

doi:10.1371/journal.pone.0006372, 2009.

875 Andersen, K. S., Kirkegaard, R. H., Karst, S. M. and Albertsen, M.: ampvis2 : an R  
package to analyse and visualise 16S rRNA amplicon data, *BioRxiv*, 10–11,  
doi:dx.doi.org/10.1101/299537, 2018.

Anderson, S. R. and Harvey, E. L.: Temporal variability and ecological interactions of  
parasitic marine Syndiniales in coastal protist communities, *mSphere*, 5(3), 1–16,  
880 doi:10.1128/msphere.00209-20, 2020.

Andrade, J. M. and Estévez-Pérez, M. G.: Statistical comparison of the slopes of two  
regression lines: A tutorial, *Anal. Chim. Acta*, 838, 1–12,  
doi:https://doi.org/10.1016/j.aca.2014.04.057, 2014.

Ansotegui, A., Sarobe, A., María Trigueros, J., Urrutxurtu, I. and Orive, E.: Size  
885 distribution of algal pigments and phytoplankton assemblages in a coastal-estuarine  
environment: Contribution of small eukaryotic algae, *J. Plankton Res.*, 25(4), 341–355,  
doi:10.1093/plankt/25.4.341, 2003.

Apprill, A., McNally, S., Parsons, R. and Weber, L.: Minor revision to V4 region SSU  
rRNA 806R gene primer greatly increases detection of SAR11 bacterioplankton, *Aquat.*  
890 *Microb. Ecol.*, 75(2), 129–137, doi:10.3354/ame01753, 2015.

Arrigo, K.: Marine microorganisms and global nutrient cycles, *Nature*, 437, 349–355,  
2005.

Bakun, A.: Linking climate to population variability in marine ecosystems characterized  
by non-simple dynamics: Conceptual templates and schematic constructs, *J. Mar. Syst.*,  
895 79(3–4), 361–373, doi:10.1016/j.jmarsys.2008.12.008, 2010.

Berman-Frank, I. and Rahav, E.: Dinitrogen fixation as a source for new production in  
the Mediterranean Sea: A review., 2012.

Berman, T., Townsend, D. and Elsayed, S.: Optical transparency, chlorophyll and  
primary productivity in the eastern Mediterranean near the Israeli coast, *Oceanol. Acta*,  
900 7(3), 367–372, 1984.



- Billen, G., Servais, P. and Becquevort, S.: Dynamics of bacterioplankton in oligotrophic and eutrophic aquatic environments: bottom-up or top-down control?, *Hydrobiologia*, 207(1), 37–42, doi:10.1007/BF00041438, 1990.
- Bolyen, E., Rideout, J. R., Dillon, M. R., Bokulich, N. A., Abnet, C. C., Al-Ghalith, G. A., Alexander, H., Alm, E. J., Arumugam, M., Asnicar, F., Bai, Y., Bisanz, J. E., Bittinger, K., Brejnrod, A., Brislawn, C. J., Brown, C. T., Callahan, B. J., Caraballo-Rodríguez, A. M., Chase, J., Cope, E. K., Da Silva, R., Diener, C., Dorrestein, P. C., Douglas, G. M., Durall, D. M., Duvallet, C., Edwardson, C. F., Ernst, M., Estaki, M., Fouquier, J., Gauglitz, J. M., Gibbons, S. M., Gibson, D. L., Gonzalez, A., Gorlick, K., Guo, J., Hillmann, B., Holmes, S., Holste, H., Huttenhower, C., Huttley, G. A., Janssen, S., Jarmusch, A. K., Jiang, L., Kaehler, B. D., Kang, K. Bin, Keefe, C. R., Keim, P., Kelley, S. T., Knights, D., Koester, I., Kosciulek, T., Kreps, J., Langille, M. G. I., Lee, J., Ley, R., Liu, Y. X., Loftfield, E., Lozupone, C., Maher, M., Marotz, C., Martin, B. D., McDonald, D., McIver, L. J., Melnik, A. V., Metcalf, J. L., Morgan, S. C., Morton, J. T., Naimey, A. T., Navas-Molina, J. A., Nothias, L. F., Orchanian, S. B., Pearson, T., Peoples, S. L., Petras, D., Preuss, M. L., Priesse, E., Rasmussen, L. B., Rivers, A., Robeson, M. S., Rosenthal, P., Segata, N., Shaffer, M., Shiffer, A., Sinha, R., Song, S. J., Spear, J. R., Swafford, A. D., Thompson, L. R., Torres, P. J., Trinh, P., Tripathi, A., Turnbaugh, P. J., Ul-Hasan, S., van der Hooft, J. J. J., Vargas, F., Vázquez-Baeza, Y., Vogtmann, E., von Hippel, M., et al.: Reproducible, interactive, scalable and extensible microbiome data science using QIIME 2, *Nat. Biotechnol.*, 37(8), 852–857, doi:10.1038/s41587-019-0209-9, 2019.
- Bonnet, D. and Frid, C.: Seven copepod species considered as indicators of water-mass influence and changes: Results from a Northumberland coastal station, *ICES J. Mar. Sci.*, 61(4), 485–491, doi:10.1016/j.icesjms.2004.03.005, 2004.
- Calbet, A., Alcaraz, M., Saiz, E., Estrada, M. and Trepát, I.: Planktonic herbivorous food webs in the catalan sea (NW Mediterranean): Temporal variability and comparison of indices of phyto-zooplankton coupling based on state variables and rate processes, *J. Plankton Res.*, 18(12), 2329–2347, doi:10.1093/plankt/18.12.2329, 1996.
- Callahan, B. J., McMurdie, P. J., Rosen, M. J., Han, A. W., Johnson, A. J. A. and

- Holmes, S. P.: DADA2: High-resolution sample inference from Illumina amplicon data, *Nat. Methods*, 13(7), 581–583, doi:10.1038/nmeth.3869, 2016.
- Campbell, L. and Vaulot, D.: Photosynthetic picoplankton community structure in the subtropical North Pacific Ocean near Hawaii (station ALOHA), *Deep Sea Res. Part I*  
935 *Oceanogr. Res. Pap.*, 40(10), 2043–2060, doi:10.1016/0967-0637(93)90044-4, 1993.
- Christaki, U.: Nanoflagellate predation on auto- and heterotrophic picoplankton in the oligotrophic Mediterranean Sea, *J. Plankton Res.*, 23(11), 1297–1310, doi:10.1093/plankt/23.11.1297, 2001.
- Christaki, U., Van Wambeke, F., Lefevre, D., Lagaria, a., Prieur, L., Pujo-Pay, M.,  
940 Grattepanche, J.-D., Colombet, J., Psarra, S., Dolan, J. R., Sime-Ngando, T., Conan, P., Weinbauer, M. G. and Moutin, T.: Microbial food webs and metabolic state across oligotrophic waters of the Mediterranean Sea during summer, *Biogeosciences*, 8(7), 1839–1852, doi:10.5194/bg-8-1839-2011, 2011.
- Christou, E. D.: Interannual variability of copepods in a Mediterranean coastal area  
945 (Saronikos Gulf, Aegean Sea), *J. Mar. Syst.*, 15(1–4), 523–532, doi:10.1016/S0924-7963(97)00080-8, 1998.
- Christou, E. D., Siokou-frangou, I., Mazzocchi, M. G. and Aguzzi, L.: Mesozooplankton abundance in the eastern Mediterranean during spring 1992, in *Rapports et Proces-Verbaux des Reunions – Commission Internationale pour l’Exploration Scientifique de la*  
950 *Mer M’editerran’ee.*, vol. 35, pp. 410–411., 1998.
- Church, M. J., Mahaffey, C., Letelier, R. M., Lukas, R., Zehr, J. P. and Karl, D. M.: Physical forcing of nitrogen fixation and diazotroph community structure in the North Pacific subtropical gyre, *Global Biogeochem. Cycles*, 23(2), doi:10.1029/2008GB003418, 2009.
- 955 Clarke, L. J., Bestley, S., Bissett, A. and Deagle, B. E.: A globally distributed *Syndiniales* parasite dominates the Southern Ocean micro-eukaryote community near the sea-ice edge, *ISME J.*, 13(3), 734–737, doi:10.1038/s41396-018-0306-7, 2019.
- Coats, D. W. and Park, M. G.: Parasitism of photosynthetic dinoflagellates by three

strains of *Amoebophrya* (Dinophyta): Parasite survival, infectivity, generation time, and  
 960 host specificity, *J. Phycol.*, 38(3), 520–528, doi:10.1046/j.1529-8817.2002.01200.x,  
 2002.

Cole, J., Findlay, S. and Pace, M.: Bacterial production in fresh and saltwater ecosystems  
 - A cross-system overview, *Mar. Ecol. Prog. Ser.*, 43(1–2), 1–10, 1988.

Colgan, D. J., Hutchings, P. A. and Braune, M.: A multigene framework for polychaete  
 965 phylogenetic studies, *Org. Divers. Evol.*, 6(3), 220–235, doi:10.1016/j.ode.2005.11.002,  
 2006.

Condie, S. and Condie, R.: Retention of plankton within ocean eddies, *Glob. Ecol.  
 Biogeogr.*, 25(10), 1264–1277, doi:10.1111/geb.12485, 2016.

Denis, M., Thyssen, M., Martin, V., Manca, B. and Vidussi, F.: Ultraphytoplankton  
 970 basin-scale distribution in the eastern Mediterranean Sea in winter: link to  
 hydrodynamism and nutrients, *Biogeosciences*, 7, 2227–2244, doi:10.5194/bg-7-2227-  
 2010, 2010.

Dishon, G., Dubinsky, Z., Caras, T., Rahav, E., Bar-Zeev, E., Tzuber, Y. and Iluz, D.:  
 Optical habitats of ultraphytoplankton groups in the Gulf of Eilat (Aqaba), Northern Red  
 975 Sea, *Int. J. Remote Sens.*, 33(9), 2683–2705, doi:10.1080/01431161.2011.619209, 2012.

Djaoudi, K., Van Wambeke, F., Coppola, L., D’Ortenzio, F., Helias-Nunige, S.,  
 Raimbault, P., Taillandier, V., Testor, P., Wagener, T. and Pulido-Villena, E.: Sensitive  
 Determination of the Dissolved Phosphate Pool for an Improved Resolution of Its  
 Vertical Variability in the Surface Layer: New Views in the P-Depleted Mediterranean  
 980 Sea, *Front. Mar. Sci.*, 5(July), 1–11, doi:10.3389/fmars.2018.00234, 2018.

Dolan, J. R. and Marrasé, C.: Planktonic ciliate distribution relative to a deep chlorophyll  
 maximum: Catalan Sea, N.W. Mediterranean, June 1993, *Deep. Res. Part I*, 42(11–12),  
 1965–1987, doi:10.1016/0967-0637(95)00092-5, 1995.

Dolan, J. R., Claustre, H., Carlotti, F., Plounevez, S. and Moutin, T.: Microzooplankton  
 985 diversity: Relationships of tintinnid ciliates with resources, competitors and predators  
 from the Atlantic Coast of Morocco to the Eastern Mediterranean, *Deep. Res. Part I*

- Oceanogr. Res. Pap., 49(7), 1217–1232, doi:10.1016/S0967-0637(02)00021-3, 2002.
- Duarte, C. M., Duarte, C. M., Regaudie-de-jioux, A. and Agust, S.: The oligotrophic ocean is heterotrophic, *Ann. Rev. Mar. Sci.*, 5(June 2014), 551–569, doi:10.1146/annurev-marine-121211-172337, 2013.
- 990 Ducklow, H. W.: Bacterial production and biomass in the ocean., 1992.
- Dufois, F., Hardman-Mountford, N. J., Greenwood, J., Richardson, A. J., Feng, M. and Matear, R. J.: Anticyclonic eddies are more productive than cyclonic eddies in subtropical gyres because of winter mixing, *Sci. Adv.*, 2(5), 1–7, doi:10.1126/sciadv.1600282, 2016.
- 995 Dyhrman, S. T., Jenkins, B. D., Rynearson, T. A., Saito, M. A., Mercier, M. L., Alexander, H., Whitney, L. P., Drzewianowski, A., Bulygin, V. V., Bertrand, E. M., Wu, Z., Benitez-nelson, C. and Heithoff, A.: The Transcriptome and Proteome of the Diatom *Thalassiosira pseudonana* Reveal a Diverse Phosphorus Stress Response, *PLoS One*, 7(3), e33768, doi:10.1371/journal.pone.0033768, 2012.
- 1000 Efrati, S., Lehahn, Y., Rahav, E., Kress, N., Herut, B., Gertman, I., Goldman, R., Ozer, T., Lazar, M. and Heifetz, E.: Intrusion of coastal waters into the pelagic eastern Mediterranean: In situ and satellite-based characterization, *Biogeosciences*, 10(5), doi:10.5194/bg-10-3349-2013, 2013.
- 1005 Falkowski, P. G., Ziemann, D., Kolber, Z. and Bienfang, P. K.: Role of eddy pumping in enhancing primary production in the ocean, *Nature*, 352(6330), 55–58, doi:10.1038/352055a0, 1991.
- Falkowski, P. G., Laws, E. A., Barber, R. T. and Murray, J. W.: Phytoplankton and Their Role in Primary, New, and Export Production, in *Ocean Biogeochemistry*, pp. 99–121, Springer Berlin Heidelberg, Berlin, Heidelberg., 2003.
- 1010 Feliú, G., Pagano, M., Hidalgo, P. and Carlotti, F.: Structure and functioning of epipelagic mesozooplankton and response to dust events during the spring PEACETIME cruise in the Mediterranean Sea, *Biogeosciences Discuss.*, (30), 1–35, doi:10.5194/bg-2020-126, 2020.

- 1015 Fong, A. A., Karl, D. M., Lukas, R., Letelier, R. M., Zehr, J. P. and Church, M. J.: Nitrogen fixation in an anticyclonic eddy in the oligotrophic North Pac, *ISME J.*, 2(6), 663–676, doi:10.1038/ismej.2008.22, 2008.
- Frangoulis, C., Christou, E. D. and Hecq, J. H.: Comparison of marine copepod outfluxes: Nature, rate, fate and role in the carbon and nitrogen cycles., 2004.
- 1020 Gasol, J. M., Del Giorgio, P. A. and Duarte, C. M.: Biomass distribution in marine planktonic communities, *Limnol. Oceanogr.*, 42(6), 1353–1363, doi:10.4319/lo.1997.42.6.1353, 1997.
- Gaube, P., McGillicuddy, D. J., Chelton, D. B., Behrenfeld, M. J. and Strutton, P. G.: Regional variations in the influence of mesoscale eddies on near-surface chlorophyll, *J. Geophys. Res. Ocean.*, 119(12), 8195–8220, doi:10.1002/2014JC010111, 2014.
- 1025 Geider, R. J. and La Roche, J.: Redfield revisited: Variability of C:N:P in marine microalgae and its biochemical basis, *Eur. J. Phycol.*, 37(1), 1–17, doi:10.1017/S0967026201003456, 2002.
- Gershwin, L. ann, Richardson, A. J., Winkel, K. D., Fenner, P. J., Lippmann, J., Hore, R., 1030 Avila-Soria, G., Brewer, D., Kloser, R. J., Steven, A. and Condie, S.: *Biology and Ecology of Irukandji Jellyfish (Cnidaria: Cubozoa)*, 1st ed., Elsevier Ltd., 2013.
- Goldthwait, S. A. and Steinberg, D. K.: Elevated biomass of mesozooplankton and enhanced fecal pellet flux in cyclonic and mode-water eddies in the Sargasso Sea, *Deep. Res. Part II Top. Stud. Oceanogr.*, 55(10–13), 1360–1377, doi:10.1016/j.dsr2.2008.01.003, 2008.
- 1035 Griffin, S. L. and Rippingale, R. J.: Zooplankton grazing dynamics: Top-down control of phytoplankton and its relationship to an estuarine habitat, *Hydrol. Process.*, 15(13), 2453–2464, doi:10.1002/hyp.293, 2001.
- Groom, S., Herut, B., Brenner, S., Zodiatis, G., Psarra, S., Kress, N., Krom, M. D., Law, 1040 C. S. and Drakopoulos, P.: Satellite-derived spatial and temporal biological variability in the Cyprus Eddy, *Deep Sea Res. Part II Top. Stud. Oceanogr.*, 52(22–23), 2990–3010, doi:10.1016/j.dsr2.2005.08.019, 2005.

- Guillou, L., Viprey, M., Chambouvet, A., Welsh, R. M., Kirkham, A. R., Massana, R., Scanlan, D. J. and Worden, A. Z.: Widespread occurrence and genetic diversity of marine parasitoids belonging to Syndiniales (Alveolata), *Environ. Microbiol.*, 10(12), 3349–3365, doi:10.1111/j.1462-2920.2008.01731.x, 2008.
- Guixa-Boixereu, N., Vaqué, D., Gasol, J. M. and Pedrós-Alió, C.: Distribution of viruses and their potential effect on bacterioplankton in an oligotrophic marine system, *Aquat. Microb. Ecol.*, 19(3), 205–213, doi:10.3354/ame019205, 1999a.
- Guixa-Boixereu, N., Lysnes, K., Guixa-boixereu, R. I. A. and Lysnes, K.: Viral lysis and bacterivory during a phytoplankton bloom in a coastal water microcosm, *Appl. Environ. Microbiol.*, 65(5), 1949–1958, 1999b.
- Gundersen, K., Heldal, M., Norland, S., Purdie, D. A. and Knap, A. H.: Elemental C, N, and P cell content of individual bacteria collected at the Bermuda Atlantic Time-series Study (BATS) site, *Limnol. Oceanogr.*, 47(5), 1525–1530, doi:10.4319/lo.2002.47.5.1525, 2002.
- [Harris, R., Wiebe, P., Lenz, J., Skjoldal, H.R. and Huntley, M. eds., 2000. ICES zooplankton methodology manual. Elsevier.](#)
- Hazan, O., Silverman, J., Sisma-Ventura, G., Ozer, T., Gertman, I., Shoham-Frider, E., Kress, N. and Rahav, E.: Mesopelagic prokaryotes alter surface phytoplankton production during simulated deep mixing experiments in Eastern Mediterranean Sea waters, *Front. Mar. Sci.*, 5, doi:10.3389/fmars.2018.00001, 2018.
- Heller, P., Casaletto, J., Ruiz, G. and Geller, J.: Data Descriptor: A database of metazoan cytochrome c oxidase subunit I gene sequences derived from GenBank with CO-ARBitrator, *Sci. Data*, 5, 1–7, doi:10.1038/sdata.2018.156, 2018.
- Hernández-León, S., Almeida, C., Gómez, M., Torres, S., Montero, I. and Portillo-Hahnefeld, A.: Zooplankton biomass and indices of feeding and metabolism in island-generated eddies around Gran Canaria, *J. Mar. Syst.*, 30(1–2), 51–66, doi:10.1016/S0924-7963(01)00037-9, 2001.
- Herut, B., Collier, R. and Krom, M. D.: The role of dust in supplying nitrogen and

- phosphorus to the southeast Mediterranean, *Limnol. Oceanogr.*, 47(3), 870–878, doi:10.4319/lo.2002.47.3.0870, 2002.
- Herut, B., Zohary, T., Krom, M. D. D., Mantoura, R. F. C., Pitta, P., Psarra, S., Rassoulzadegan, F., Tanaka, T. and Frede Thingstad, T.: Response of East Mediterranean surface water to Saharan dust: On-board microcosm experiment and field observations, *Deep. Res. Part II Top. Stud. Oceanogr.*, 52(22–23), 3024–3040, doi:10.1016/j.dsr2.2005.09.003, 2005.
- Holliday, D., Beckley, L. E. and Olivar, M. P.: Incorporation of larval fishes into a developing anti-cyclonic eddy of the Leeuwin Current off south-western Australia, *J. Plankton Res.*, 33(11), 1696–1708, doi:10.1093/plankt/fbr064, 2011.
- Houlbrèque, F., Delesalle, B., Blanchot, J., Montel, Y. and Ferrier-Pagès, C.: Picoplankton removal by the coral reef community of La Prévoyante, Mayotte Island, *Aquat. Microb. Ecol.*, 44(1), 59–70, doi:10.3354/ame044059, 2006.
- Huggett, J. A.: Mesoscale distribution and community composition of zooplankton in the Mozambique Channel, *Deep. Res. Part II Top. Stud. Oceanogr.*, 100, 119–135, doi:10.1016/j.dsr2.2013.10.021, 2014.
- Ignatiades, L., Psarra, S., Zervakis, V., Pagou, K., Souvermezoglou, E., Assimakopoulou, G. and Gotsis-Skretas, O.: Phytoplankton size-based dynamics in the Aegean Sea (Eastern Mediterranean), *J. Mar. Syst.*, 36(1–2), 11–28, doi:10.1016/S0924-7963(02)00132-X, 2002.
- Ikeda, T.: Metabolic rates of epipelagic marine zooplankton as a function of body mass and temperature, *Mar. Biol.*, 85(1), 1–11, doi:10.1007/BF00396409, 1985.
- Ikeda, T., Torres, J. J., Hernandez-Leon, S. and Geiger, S. P.: Metabolism, in *ICES zooplankton methodology manual*, edited by R. Harris, pp. 455–532, Academic Press, London., 2000.
- Ioannou, A., Stegner, A., Tuel, A., LeVu, B., Dumas, F. and Speich, S.: Cyclostrophic Corrections of AVISO/DUACS Surface Velocities and Its Application to Mesoscale Eddies in the Mediterranean Sea, *J. Geophys. Res. Ocean.*, 124(12), 8913–8932,

doi:10.1029/2019JC015031, 2019.

- 1100 Isari, S., Somarakis, S., Christou, E. D. and Fragopoulou, N.: Summer mesozooplankton assemblages in the north-eastern Aegean Sea: The influence of Black Sea water and an associated anticyclonic eddy, *J. Mar. Biol. Assoc. United Kingdom*, 91(1), 51–63, doi:10.1017/S0025315410000123, 2011.

Isla, J. A., Ceballos, S., Huskin, I., Anadón, R. and Álvarez-Marqués, F.:

- 1105 Mesozooplankton distribution, metabolism and grazing in an anticyclonic slope water oceanic eddy (SWODDY) in the Bay of Biscay, *Mar. Biol.*, 145(6), 1201–1212, doi:10.1007/s00227-004-1408-5, 2004.

Jeffrey, S. W., Mantoura, R. F. C. and Wright, S. W.: *Phytoplankton pigments in oceanography: guidelines to modern methods*, 1st ed., edited by S. . Jeffery, R. F. C.

- 1110 Mantoura, and S. W. Wright, UNESCO, Paris., 1997.

Kirchman, D. L.: *Processes in microbial ecology*, 1st edn., edited by E. DL Kirchman, Oxford University Press, Oxford., 2012.

Koblentz-Mishke, O. ., Volrovinsky, V. G. and Kabanova, V. .: Plankton primary production of the world ocean, in *Scientific exploration of the South Pacific*, edited by

- 1115 W. . Wooster, pp. 183–193, National Academy of Sciences, Washington, DC., 1970.

[Koppelman, R., Böttger-Schnack, R., Möbius, J. and Weikert, H., 2009. Trophic relationships of zooplankton in the eastern Mediterranean based on stable isotope measurements. \*Journal of Plankton Research\*, 31\(6\), pp.669-686.](#)

Kress, N., Frede Thingstad, T., Pitta, P., Psarra, S., Tanaka, T., Zohary, T., Groom, S.,

- 1120 Herut, B., Fauzi, R., Polychronaki, T., Rassoulzadegan, F. and Spyres, G.: Effect of P and N addition to oligotrophic Eastern Mediterranean waters influenced by near-shore waters: A microcosm experiment, *Deep. Res. Part II Top. Stud. Oceanogr.*, 52(22–23), 3054–3073, doi:10.1016/j.dsr2.2005.08.013, 2005.

Kress, N., Gertman, I. and Herut, B.: Temporal evolution of physical and chemical characteristics of the water column in the Easternmost Levantine Basin (Eastern Mediterranean Sea) from 2002 to 2010, *J. Mar. Syst.*, 135, 6–13,

1125



doi:10.1016/j.jmarsys.2013.11.016, 2014.

1130 Krom, M., Kress, N., Berman-Frank, I. and Rahav, E.: Past, present and future patterns in the nutrient chemistry of the eastern mediterranean, in *The Mediterranean Sea: Its History and Present Challenges*, pp. 49–68., 2014.

1135 Krom, M. D., Woodward, E. M. S., Herut, B., Kress, N., Carbo, P., Mantoura, R. F. C., Spyres, G., Thingsted, T. F., Wassmann, P., Wexels-Riser, C., Kitidis, V., Law, C. and Zodiatis, G.: Nutrient cycling in the south east Levantine basin of the eastern Mediterranean: Results from a phosphorus starved system, *Deep. Res. Part II Top. Stud. Oceanogr.*, 52(22–23), 2879–2896, doi:10.1016/j.dsr2.2005.08.009, 2005.

Kruk, C. and Segura, A. M.: The habitat template of phytoplankton morphology-based functional groups, *Hydrobiologia*, 698(1), 191–202, doi:10.1007/s10750-012-1072-6, 2012.

1140 Landry, M. R., Brown, S. L., Rii, Y. M., Selph, K. E., Bidigare, R. R., Yang, E. J. and Simmons, M. P.: Depth-stratified phytoplankton dynamics in Cyclone Opal, a subtropical mesoscale eddy, *Deep. Res. Part II Top. Stud. Oceanogr.*, 55(10–13), 1348–1359, doi:10.1016/j.dsr2.2008.02.001, 2008a.

1145 Landry, M. R., Decima, M., Simmons, M. P., Hannides, C. C. S. and Daniels, E.: Mesozooplankton biomass and grazing responses to Cyclone Opal, a subtropical mesoscale eddy, *Deep. Res. Part II Top. Stud. Oceanogr.*, 55(10–13), 1378–1388, doi:10.1016/j.dsr2.2008.01.005, 2008b.

Lavaniegos, B. E. and Hereu, C. M.: Seasonal variation in hyperiid amphipod abundance and diversity and influence of mesoscale structures off Baja California, *Mar. Ecol. Prog. Ser.*, 394, 137–152, doi:10.3354/meps08285, 2009.

1150 Laws, E. A.: Evaluation of In Situ Phytoplankton Growth Rates : A Synthesis of Data from Varied Approaches, *Annu. Rev. Mar. Sci.*, 5, 247–268, doi:10.1146/annurev-marine-121211-172258, 2013.

Le Vu, B., Stegner, A. and Arsouze, T.: Angular momentum eddy detection and tracking algorithm (AMEDA) and its application to coastal eddy formation, *J. Atmos. Ocean.*

- Technol., 35(4), 739–762, doi:10.1175/JTECH-D-17-0010.1, 2018.
- Limer, B. D., Bloomberg, J. and Holstein, D. M.: The Influence of Eddies on Coral Larval Retention in the Flower Garden Banks, *Front. Mar. Sci.*, 7(May), 1–16, doi:10.3389/fmars.2020.00372, 2020.
- Lin, S., Litaker, R. W. and Sunda, W. G.: Phosphorus physiological ecology and molecular mechanisms in marine phytoplankton, *J. Phycol.*, 52(1), 10–36, doi:10.1111/jpy.12365, 2016.
- Ling, S. D. and Johnson, C. R.: Population dynamics of an ecologically important range-extender: Kelp beds versus sea urchin barrens, *Mar. Ecol. Prog. Ser.*, 374, 113–125, doi:10.3354/meps07729, 2009.
- Liu, H., Zhu, M., Guo, S., Zhao, X. and Sun, X.: Effects of an anticyclonic eddy on the distribution and community structure of zooplankton in the South China Sea northern slope, *J. Mar. Syst.*, 205(January), 103311, doi:10.1016/j.jmarsys.2020.103311, 2020.
- Logerwell, E. A. and Smith, P. E.: Mesoscale eddies and survival of late stage Pacific sardine (*Sardinops sagax*) larvae, *Fish. Oceanogr.*, 10(1), 13–25, doi:10.1046/j.1365-2419.2001.00152.x, 2001.
- Lomas, M. W., Bates, N. R., Johnson, R. J., Knap, A. H., Steinberg, D. K. and Carlson, C. A.: Two decades and counting: 24-years of sustained open ocean biogeochemical measurements in the Sargasso Sea, *Deep. Res. Part II Top. Stud. Oceanogr.*, 93, 16–32, doi:10.1016/j.dsr2.2013.01.008, 2013.
- López-Sandoval, D. C., Fernández, a. and Marañón, E.: Dissolved and particulate primary production along a longitudinal gradient in the Mediterranean Sea, *Biogeosciences*, 8(3), 815–825, doi:10.5194/bg-8-815-2011, 2011.
- Love, M. I., Huber, W. and Anders, S.: Moderated estimation of fold change and dispersion for RNA-seq data with DESeq2, *Genome Biol.*, 15(12), 1–21, doi:10.1186/s13059-014-0550-8, 2014.
- Ludwig, W., Dumont, E., Meybeck, M. and Heussner, S.: River discharges of water and nutrients to the Mediterranean and Black Sea: Major drivers for ecosystem changes

- during past and future decades?, *Prog. Oceanogr.*, 80(3–4), 199–217, doi:10.1016/j.pocean.2009.02.001, 2009.
- 1185 Luna, G. M., Bianchelli, S., Decembrini, F., De Domenico, E., Danovaro, R. and Dell’Anno, A.: The dark portion of the Mediterranean Sea is a bioreactor of organic matter cycling, *Global Biogeochem. Cycles*, 26(2), 1–14, doi:10.1029/2011GB004168, 2012.
- 1190 Mackas, D. L., Tsurumi, M., Galbraith, M. D. and Yelland, D. R.: Zooplankton distribution and dynamics in a North Pacific Eddy of coastal origin: II. Mechanisms of eddy colonization by and retention of offshore species, *Deep. Res. Part II Top. Stud. Oceanogr.*, 52(7–8), 1011–1035, doi:10.1016/j.dsr2.2005.02.008, 2005.
- 1195 Marañón, E., Cermeno, P. and Pérez, V.: Continuity in the photosynthetic production of dissolved organic carbon from eutrophic to oligotrophic waters, *Mar. Ecol. Prog. Ser.*, 299, 7–17, doi:10.3354/meps299007, 2005.
- 1200 Marañón, E., Van Wambeke, F., Uitz, J., Boss, E., Pérez-Lorenzo, M., Dinasquet, J., Haëntjens, N., Dimier, C., Taillandier, V. and Zäncker, B.: Deep maxima of phytoplankton biomass, primary production and bacterial production in the Mediterranean Sea during late spring, *Biogeosciences*, 18, 1749–1767, doi:10.5194/bg-18-1749-2021, 2021.
- 1205 Matis, P. A., Figueira, W. F., Suthers, I. M., Humphries, J., Miskiewicz, A., Coleman, R. A., Kelaher, B. P. and Taylor, M. D.: Cyclonic entrainment? The ichthyoplankton attributes of three major water mass types generated by the separation of the East Australian Current, *ICES J. Mar. Sci.*, 71(7), 1696–1705, doi:10.1093/icesjms/fsu062, 2014.
- Mazzocchi, M. G., Christou, E. D., Fragopoulou, N. and Siokou-frangou, I.: Mesozooplankton distribution from Sicily to Cyprus (Eastern Mediterranean): I. General aspects, *Oceanol. Acta*, 20(3), 521–535, 1997.
- 1210 McManus, G. B., Liu, W., Cole, R. A., Biemesderfer, D. and Mydosh, J. L.: *Strombidium rassoulzadegani*: A model species for chloroplast retention in Oligotrich Ciliates, *Front.*

- Mar. Sci., 5(JUN), 1–11, doi:10.3389/fmars.2018.00205, 2018.
- McMurdie, P. J. and Holmes, S.: Phyloseq: An R Package for Reproducible Interactive Analysis and Graphics of Microbiome Census Data, PLoS One, 8, e61217, doi:10.1371/journal.pone.0061217, 2013.
- 1215 Menna, M., Poulain, P.-M., Zodiatis, G. and Gertman, I.: On the surface circulation of the Levantine sub-basin derived from Lagrangian drifters and satellite altimetry data, Deep Sea Res. Part I Oceanogr. Res. Pap., 65, 46–58, doi:10.1016/j.dsr.2012.02.008, 2012.
- Mével, G., Vernet, M., Goutx, M. and Ghiglione, J. F.: Seasonal to hour variation scales in abundance and production of total and particle-attached bacteria in the open NW  
 1220 Mediterranean Sea (0-1000 m), Biogeosciences, 5(6), 1573–1586, doi:10.5194/bg-5-1573-2008, 2008.
- Miller, I., Sweatman, H., Cheal, A., Emslie, M., Johns, K., Jonker, M. and Osborne, K.: Origins and implications of a primary crown-of-thorns starfish outbreak in the southern great barrier reef, J. Mar. Biol., 2015, 1–10, doi:10.1155/2015/809624, 2015.
- 1225 Mkhinini, N., Santi Coimbra, A. L., Stegner, A., Arsouze, T., Taupier-Letage, I. and Beranger, K.: Long-lived mesoscale eddies in the eastern Mediterranean Sea: Analysis of 20 years of AVISO geostrophic velocities, J. Geophys. Res. Ocean., 119, 8603–8626, doi:10.1002/2014JC010176.Received, 2014.
- Moore, C. M., Mills, M. M., Arrigo, K. R., Berman-Frank, I., Bopp, L., Boyd, P. W.,  
 1230 Galbraith, E. D., Geider, R. J., Guieu, C., Jaccard, S. L., Jickells, T. D., La Roche, J., Lenton, T. M., Mahowald, N. M., Maranon, E., Marinov, I., Moore, J. K., Nakatsuka, T., Oschlies, A., Saito, M. A., Thingstad, T. F., Tsuda, A. and Ulloa, O.: Processes and patterns of oceanic nutrient limitation, Nat. Geosci, 6(9), 701–710, doi:10.1038/ngeo1765, 2013.
- 1235 Motoda, S., 1959. Devices of simple plankton apparatus. Memoirs of the faculty of fisheries Hokkaido University, 7(1-2), pp.73-94.
- Mullaney, T. J. and Suthers, I. M.: Entrainment and retention of the coastal larval fish assemblage by a short-lived, submesoscale, frontal eddy of the East Australian Current,

- Limnol. Oceanogr., 58(5), 1546–1556, doi:10.4319/lo.2013.58.5.1546, 2013.
- 1240 Nival, P., Nival, S. and Thiriot, A.: Influence des conditions hivernales sur les productions phyto- et zooplanctoniques en Méditerranée Nord-Occidentale. V. Biomasse et production zooplanctonique - relations phyto-zooplankton, *Mar. Biol.*, 31(3), 249–270, doi:10.1007/BF00387153, 1975.
- Olli, K., Wassmann, P., Reigstad, M., Ratkova, T. N., Arashkevich, E., Pasternak, A.,  
1245 Matrai, P. A., Knulst, J., Tranvik, L., Klais, R. and Jacobsen, A.: The fate of production in the central Arctic Ocean - top-down regulation by zooplankton expatriates?, *Prog. Oceanogr.*, 72(1), 84–113, doi:10.1016/j.pocean.2006.08.002, 2007.
- Ozer, T., Gertman, I., Kress, N., Silverman, J. and Herut, B.: Interannual thermohaline (1979–2014) and nutrient (2002–2014) dynamics in the Levantine surface and  
1250 intermediate water masses, SE Mediterranean Sea, *Glob. Planet. Change*, 151, 60–67, doi:10.1016/j.gloplacha.2016.04.001, 2017.
- Palomera, I., Olivar, M. P., Salat, J., Sabatés, A., Coll, M., García, A. and Morales-Nin, B.: Small pelagic fish in the NW Mediterranean Sea: An ecological review, *Prog. Oceanogr.*, 74(2–3), 377–396, doi:10.1016/j.pocean.2007.04.012, 2007.
- 1255 Pancucci-Papadopoulou, M.-A., Siokou-Frangou, L., Theocharis, A. and Georgopoulos, D.: Zooplankton vertical distribution in relation to the hydrology in the NW Levantine, *Oceanol. Acta*, 15(4), 365–381, 1992.
- Parada, A. E., Needham, D. M. and Fuhrman, J. A.: Every base matters: Assessing small subunit rRNA primers for marine microbiomes with mock communities, time series and  
1260 global field samples, *Environ. Microbiol.*, 18(5), 1403–1414, doi:10.1111/1462-2920.13023, 2016.
- Pasternak, A., Wassmann, P. and Riser, C. W.: Does mesozooplankton respond to episodic P inputs in the Eastern Mediterranean?, *Deep. Res. Part II Top. Stud. Oceanogr.*, 52(22–23), 2975–2989, doi:10.1016/j.dsr2.2005.09.002, 2005.
- 1265 Pinca, S. and Dallot, S.: Meso- and macrozooplankton composition patterns related to hydrodynamic structures in the Ligurian Sea (Trophos-2 experiment, April-June 1986),

- Mar. Ecol. Prog. Ser., 126(1–3), 49–65, doi:10.3354/meps126049, 1995.
- Pinca, S. and Dallot, S.: Zooplankton community structure in the Western Mediterranean sea related to mesoscale hydrodynamics, *Hydrobiologia*, 356(1–3), 127–142, doi:10.1023/a:1003151609682, 1997.
- Pitta, P., Giannakourou, A. and Christaki, U.: Planktonic ciliates in the oligotrophic Mediterranean Sea: Longitudinal trends of standing stocks, distributions and analysis of food vacuole contents, *Aquat. Microb. Ecol.*, 24(3), 297–311, doi:10.3354/ame024297, 2001.
- Pitta, P., Nejstgaard, J. C., Tsagaraki, T. M., Zervoudaki, S., Egge, J. K., Frangoulis, C., Lagaria, A., Magiopoulos, I., Psarra, S., Sandaa, R.-A., Skjoldal, E. F., Tanaka, T., Thyraug, R. and Thingstad, T. F.: Confirming the “Rapid phosphorus transfer from microorganisms to mesozooplankton in the Eastern Mediterranean Sea” scenario through a mesocosm experiment, *J. Plankton Res.*, 38(3), 502–521, doi:10.1093/plankt/fbw010, 2016.
- Pitta, P., Kanakidou, M., Mihalopoulos, N., Christodoulaki, S., Dimitriou, P. D., Frangoulis, C., Giannakourou, A., Kagiorgi, M., Lagaria, A., Nikolaou, P., Papageorgiou, N., Psarra, S., Santi, I., Tsapakis, M., Tsiola, A., Violaki, K. and Petihakis, G.: Saharan dust deposition effects on the microbial food web in the Eastern Mediterranean: A study based on a mesocosm experiment, *Front. Mar. Sci.*, 4(May), 1–19, doi:10.3389/fmars.2017.00117, 2017.
- Psarra, S., Tselepidis, A. and Ignatiades, L.: Primary productivity in the oligotrophic Cretan Sea (NE Mediterranean): seasonal and interannual variability, *Prog. Oceanogr.*, 46(2–4), 187–204, 2000.
- Pujo-Pay, M., Conan, P., Oriol, L., Cornet-Barthaux, V., Falco, C., Ghiglione, J. F., Goyet, C., Moutin, T. and Prieur, L.: Integrated survey of elemental stoichiometry (C, N, P) from the western to eastern Mediterranean Sea, *Biogeosciences*, 8(4), 883–899, doi:10.5194/bg-8-883-2011, 2011.
- Pulido-Villena, E., Ghiglione, J. F., Ortega-Retuerta, E., Van-Wambeke, F. and Zohary,

- 1295 T.: Heterotrophic bacteria in the pelagic realm of the Mediterranean Sea, in *Life in the Mediterranean Sea: A Look at Habitat Changes*, pp. 227–265, Nova Science Publishers, NY., 2012.
- R Core Team: R: A Language and Environment for Statistical Computing, 2018.
- 1300 Rabi, C., Rilov, G., Morov, A. R. and Guy-Haim, T.: First record of the red sea gastropod *nerita sanguinolenta* menke, 1829 (Gastropoda: Cycloneritida: Neritidae) from the israeli mediterranean coast, *BioInvasions Rec.*, 9(3), 496–503, doi:10.3391/bir.2020.9.3.06, 2020.
- 1305 Rahav, E., Herut, B., Stambler, N., Bar-Zeev, E., Mulholland, M. R. and Berman-Frank, I.: Uncoupling between dinitrogen fixation and primary productivity in the eastern Mediterranean Sea, *J. Geophys. Res. Biogeosciences*, 118(1), 195–202, doi:10.1002/jgrg.20023, 2013.
- Rahav, E., Silverman, J., Raveh, O., Hazan, O., Rubin-Blum, M., Zeri, C., Gogou, A., Kralj, M., Pavlidou, A. and Kress, N.: The deep water of Eastern Mediterranean Sea is a hotspot for bacterial activity, *Deep Sea Res. Part II Top. Stud. Oceanogr.*, doi:10.1016/j.dsr2.2019.03.004, 2019.
- 1310 Rahav, E., Herut, B., Spungin, D., Levi, A., Mulholland, M. R. and Berman-frank, I.: Heterotrophic bacteria outcompete diazotrophs for orthophosphate in the Mediterranean Sea, *Limnol. Oceanogr.*, 9999, 1–13, doi:10.1002/lno.11983, 2021.
- 1315 Rakesh, M., Raman, A. V., Kalavati, C., Subramanian, B. R., Sharma, V. S., Sunitha Babu, E. and Sateesh, N.: Zooplankton community structure across an eddy-generated upwelling band close to a tropical bay-mangrove ecosystem, *Mar. Biol.*, 154(6), 953–972, doi:10.1007/s00227-008-0991-2, 2008.
- Reich, T., Ben-Ezra, T., Belkin, N., Tsemel, A., Aharonovich, D., Roth-Rosenberg, D., Givati, S., Bialik, O., Herut, B., Berman-Frank, I., Frada, M., Krom, M. D., Lehahn, Y., 1320 Rahav, E. and Sher, D.: ~~Seasonal~~ A year in the life of the Eastern Mediterranean Sea: Monthly dynamics of phytoplankton and bacterioplankton ~~at the in an~~ in an ultra-oligotrophic ~~southeastern Mediterranean Sea, bioRxiv, 2021.03.24.436734, sea. Deep Sea Research I~~

[182 \(2022\) 103720. https://doi.org/10.1101/2021.03.24.436734](https://doi.org/10.1101/2021.03.24.436734),  
[2021.1016/j.dsr.2022.103720](https://doi.org/10.1016/j.dsr.2022.103720).

- 1325 Riandey, V., Champalbert, G., Carlotti, F., Taupier-Letage, I. and Thibault-Botha, D.:  
 Zooplankton distribution related to the hydrodynamic features in the Algerian Basin  
 (western Mediterranean Sea) in summer 1997, *Deep. Res. Part I Oceanogr. Res. Pap.*,  
 52(11), 2029–2048, doi:10.1016/j.dsr.2005.06.004, 2005.
- Ridame, C., Le Moal, M., Guieu, C., Ternon, E., Biegala, I. C., L'Helguen, S. and Pujo-  
 1330 Pay, M.: Nutrient control of N<sub>2</sub> fixation in the oligotrophic Mediterranean Sea and the  
 impact of Saharan dust events, *Biogeosciences Discuss.*, 8(2), 2629–2657,  
 doi:10.5194/bgd-8-2629-2011, 2011.
- Robinson, A. R. and Golnaraghi, M.: The physical and dynamical oceanography of the  
 Eastern Mediterranean Sea, in *Ocean Processes in Climate Dynamics: Global and*  
 1335 *Mediterranean Examples*, edited by P. Malanotte-Rizzoli and A. R. Robinson, pp. 255–  
 306, Springer Netherlands, Dordrecht., 1994.
- Sala, M. M., Peters, F., Gasol, J. M., Pedrós-Alió, C., Marrasé, C. and Vaqué, D.:  
 Seasonal and spatial variations in the nutrient limitation of bacterioplankton growth in the  
 northwestern Mediterranean, *Aquat. Microb. Ecol.*, 27(1), 47–56,  
 1340 doi:10.3354/ame027047, 2002.
- Santi, I., Kasapidis, P., Psarra, S., Assimakopoulou, G., Pavlidou, A., Protopapa, M.,  
 Tsiola, A., Zeri, C. and Pitta, P.: Composition and distribution patterns of eukaryotic  
 microbial plankton in the ultra-oligotrophic Eastern Mediterranean Sea , *Aquat. Microb.*  
*Ecol.*, 84, 155–173, 2020.
- 1345 Sathyendranath, S. and Platt, T.: Spectral effects in bio-optical control on the ocean  
 system, *Oceanologia*, 49(1), 5–39, 2007.
- Seguin, G., Errhif, A. and Dallot, S.: Diversity and structure of pelagic copepod  
 populations in the frontal zone of the eastern Alboran sea, *Hydrobiologia*, 292–293(1),  
 369–377, doi:10.1007/BF00229962, 1994.
- 1350 Sherr, E. B. and Sherr, B. F.: Heterotrophic dinoflagellates: A significant component of



- microzooplankton biomass and major grazers of diatoms in the sea, *Mar. Ecol. Prog. Ser.*, 352, 187–197, doi:10.3354/meps07161, 2007.
- Simon, M., Alldredge, A. and Azam, F.: Protein-content and protein-synthesis rates of planktonic marine-bacteria, *Mar. Ecol. Prog. Ser.*, 51(3), 201–213, 1989.
- 1355 Siokou-Frangou, I.: Epipelagic mesozooplankton and copepod grazing along an east–west transect in the Mediterranean Sea., 2004.
- Siokou-Frangou, I., Christou, E. D., Gotsis-Scretas, O., Kontoyiannis, H., Krasakopoulou, E., Pagou, K., Pavlidou, A., Souvermezoglou, E. and Theocharis, A.: Impact of physical processes upon chemical and biological properties in the Rhodes gyre area, in *International Conference: Progress in Oceanography of the Mediterranean Sea*, 1360 Rome, November, pp. 17–19., 1997.
- Siokou-Frangou, I., Bianchi, M., Christaki, U., Christou, E. D., Giannakourou, A., Gotsis, O., Ignatiades, L., Pagou, K., Pitta, P., Psarra, S., Souvermezoglou, E., Van Wambeke, F. and Zervakis, V.: Carbon flow in the planktonic food web along a gradient of oligotrophy 1365 in the Aegean Sea (Mediterranean Sea), *J. Mar. Syst.*, 33–34, 335–353, doi:10.1016/S0924-7963(02)00065-9, 2002.
- Siokou-Frangou, I., Christaki, U., Mazzocchi, M. G., Montresor, M., Ribera d’Alcalá, M., Vaqué, D. and Zingone, a.: Plankton in the open Mediterranean Sea: a review, *Biogeosciences*, 7(5), 1543–1586, doi:10.5194/bg-7-1543-2010, 2010.
- 1370 Sisma-Ventura, G. and Rahav, E.: DOP Stimulates Heterotrophic Bacterial Production in the Oligotrophic Southeastern Mediterranean Coastal Waters, *Front. Microbiol.*, 10, 1913, doi:10.3389/fmicb.2019.01913, 2019.
- Smith, D. C., Smith, D. C., Azam, F. and Azam, F.: A simple, economical method for measuring bacterial protein synthesis rates in seawater using <sup>3</sup>H-leucine, *Mar. Microb. food web*, 6(2), 107–114, 1992. 1375
- Stambler, N.: Underwater light field of the Mediterranean Sea, in *Life in the Mediterranean Sea: A Look at Habitat Changes*, edited by N. Stambler, pp. 1–739, Nova Science Publishers., 2012.

- 1380 Steemann-Nielsen, E.: The use of radioactive carbon ( $^{14}\text{C}$ ) for measuring organic  
production in the sea, *J. des Cons. Int. Pour Explor. la Mer*, 18, 117–140, 1952.
- Stergiou, K. I., Christou, E. D. and Petrakis, G.: Modelling and forecasting monthly  
fisheries catches: Comparison of regression, univariate and multivariate time series  
methods, *Fish. Res.*, 29(1), 55–95, doi:10.1016/S0165-7836(96)00482-1, 1997.
- 1385 Strzelecki, J., Koslow, J. A. and Waite, A.: Comparison of mesozooplankton  
communities from a pair of warm- and cold-core eddies off the coast of Western  
Australia, *Deep. Res. Part II Top. Stud. Oceanogr.*, 54(8–10), 1103–1112,  
doi:10.1016/j.dsr2.2007.02.004, 2007.
- Suzuki, N., Ogane, K., Aita, Y., Kato, M., Sakai, S., Kurihara, T., Matsuoka, A.,  
Ohtsuka, S., Go, A., Nakaguchi, K., Yamaguchi, S., Takahashi, T. and Tuji, A.:  
1390 Distribution patterns of the radiolarian nuclei and symbionts using DAPI-fluorescence,  
*Bull Natl Mus Nat Sci Ser B*, 35(4), 169–182, 2009.
- Tanaka, T., Thingstad, T. F., Christaki, U., Colombet, J., Cornet-Barthaux, V., Courties,  
C., Grattepanche, J.-D., Lagaria, a., Nedoma, J., Oriol, L., Psarra, S., Pujo-Pay, M. and  
Van Wambeke, F.: Lack of P-limitation of phytoplankton and heterotrophic prokaryotes  
1395 in surface waters of three anticyclonic eddies in the stratified Mediterranean Sea,  
*Biogeosciences*, 8(2), 525–538, doi:10.5194/bg-8-525-2011, 2011.
- Thingstad, T. F., Krom, M. D., Mantoura, R. F. C., Flaten, G. a F., Groom, S., Herut, B.,  
Kress, N., Law, C. S., Pasternak, a, Pitta, P., Psarra, S., Rassoulzadegan, F., Tanaka, T.,  
Tselepidis, A., Wassmann, P., Woodward, E. M. S., Riser, C. W., Zodiatis, G. and  
1400 Zohary, T.: Nature of phosphorus limitation in the ultraoligotrophic eastern  
Mediterranean., *Science*, 309(5737), 1068–71, doi:10.1126/science.1112632, 2005.
- Tsiola, A., Tsagaraki, T. M., Giannakourou, A., Nikolioudakis, N., Yücel, N., Herut, B.  
and Pitta, P.: Bacterial growth and mortality after deposition of Saharan dust and mixed  
aerosols in the Eastern Mediterranean Sea: a mesocosm experiment., *Front. Mar. Sci.*,  
1405 3(January), 1–13, doi:10.3389/fmars.2016.00281, 2017.
- Vaillancourt, R. D., Marra, J., Seki, M. P., Parsons, M. L. and Bidigare, R. R.: Impact of

- a cyclonic eddy on phytoplankton community structure and photosynthetic competency in the subtropical North Pacific Ocean, *Deep Sea Res. Part I Oceanogr. Res. Pap.*, 50(7), 829–847, doi:10.1016/S0967-0637(03)00059-1, 2003.
- 1410 Vandromme, P., Stemann, L., Berline, L., Gasparini, S., Mousseau, L., Prejger, F., Passafiume, O., Guarini, J. M. and Gorsky, G.: Inter-annual fluctuations of zooplankton communities in the Bay of Villefranche-sur-mer from 1995 to 2005 (Northern Ligurian Sea, France), *Biogeosciences*, 8(11), 3143–3158, doi:10.5194/bg-8-3143-2011, 2011.
- 1415 Van Ruth, P., Redondo Rodriguez, A., Davies, C. and Richardson, A. J.: Indicators of depth layers important to phytoplankton production., 2020.
- Van Wambeke, F., Christaki, U., Giannakourou, A., Moutin, T., Souvermezoglou, E. and Giannokourou, A.: Longitudinal and vertical trends of bacterial limitation by phosphorus and carbon in the Mediterranean Sea, *Microb. Ecol.*, 43(1), 119–133, 2002.
- 1420 Waite, A. M., Thompson, P. A., Pesant, S., Feng, M., Beckley, L. E., Domingues, C. M., Gaughan, D., Hanson, C. E., Holl, C. M., Koslow, T., Meuleners, M., Montoya, J. P., Moore, T., Muhling, B. A., Paterson, H., Rennie, S., Strzelecki, J. and Twomey, L.: The Leeuwin Current and its eddies: An introductory overview, *Deep Sea Res. Part II Top. Stud. Oceanogr.*, 54(8), 789–796, doi:https://doi.org/10.1016/j.dsr2.2006.12.008, 2007.
- 1425 Welschmeyer, N. A.: Fluorometric analysis of chlorophyll a in the presence of chlorophyll b and pheopigments, *Limnol. Oceanogr.*, 39(8), 1985–1992, 1994.
- Wickham, H.: *Ggplot2*, Wiley Interdiscip. Rev. Comput. Stat., 3(2), 180–185, doi:10.1002/wics.147, 2011.
- 1430 Zhou, M., Carlotti, F. and Zhu, Y.: A size-spectrum zooplankton closure model for ecosystem modelling, *J. Plankton Res.*, 32(8), 1147–1165, doi:10.1093/plankt/fbq054, 2010.
- Zohary, T. and Robarts, R. R. D.: Experimental study of microbial P limitation in the eastern Mediterranean, *Limnol. Oceanogr.*, 43(3), 387–395, doi:10.4319/lo.1998.43.3.0387, 1998.
- Zohary, T., Herut, B., Krom, M. D., Fauzi C. Mantoura, R., Pitta, P., Psarra, S.,

- 1435 Rassoulzadegan, F., Stambler, N., Tanaka, T., Frede Thingstad, T. and Malcolm S. Woodward, E.: P-limited bacteria but N and P co-limited phytoplankton in the Eastern Mediterranean - A microcosm experiment, *Deep. Res. Part II Top. Stud. Oceanogr.*, 52(22–23), 3011–3023, doi:10.1016/j.dsr2.2005.08.011, 2005.